AD-A174 628 GEOMETRIC SPECKLE REDUCTION(U) ENVIRONMENTAL RESEARCH INST OF MICHIGAN ANN ARBOR T R CRIMMINS OCT 86 DAAG29-84-K-0204 1/1

UNCLASSIFIED F/G 17/9 NL

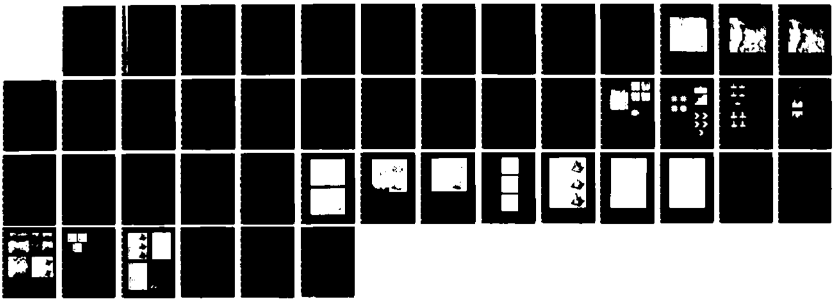

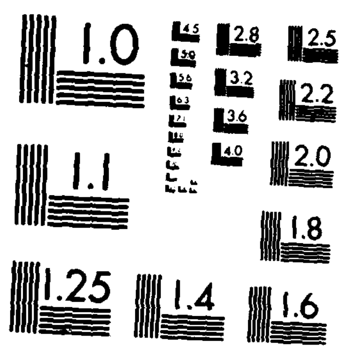

MICROCOPY RESOLUTION TEST CHART
NATIONAL BUREAU OF STANDARDS-1963-A

178100-6-F

AD-A174 628

Final Report

GEOMETRIC SPECKLE REDUCTION

THOMAS R. CRIMMINS

OCTOBER 1986

Approved for public release,
distribution unlimited.

U.S. Army Research Office
Physics Division
P.O. Box 12211
Research Triangle Park, NC 27709

Contract No. DAAG29-84-K-0204

ENVIRONMENTAL
RESEARCH INSTITUTE OF MICHIGAN
BOX 8618 • ANN ARBOR • MICHIGAN 48107

12 02 055

TABLE OF CONTENTS

LIST OF TABLES

LIST OF FIGURES

1
INTRODUCTION

The presence of speckle in imagery produced with coherent illumination (e.g., synthetic aperture radar) reduces the detectability of objects in the images [1-9]. It also reduces the effectiveness of some computer algorithms (e.g., edge detection) designed for automatic image analysis.

Thus it is desirable to reduce speckle in synthetic aperture radar (SAR) images both to assist radar image interpreters and to preprocess images for automatic recognition algorithms on computers. The goal is to smooth out the speckle but at the same time preserve features of interest like edges, strong returns, etc.

2
SUMMARY

2.1 THE GEOMETRIC FILTER

A non-linear filter was developed to reduce speckle in SAR imagery while at the same time preserving spatial information. This filter is fundamentally different from any of the speckle reduction techniques that have appeared in the literature [10-33]. It is based on geometric concepts ([34] - Appendix A), and is referred to as the geometric filter.

The original geometric filter was designed for 8-bit imagery. It is an iterative algorithm and generally about four to ten iterations is optimal although just two or three iterations will reduce the speckle significantly.

This 8-bit filter was originally implemented on a De Anza IP5500 digital video processor using a VAX 11/980 as a host system. Running time was about 14 s per iteration for 512 x 512 images. It was later implemented on a 4-stage configuration of the CYTO-HSS High Speed Cytocomputer System (recently developed at ERIM - see [46]) and running time was reduced to 0.2 s per iteration for images of the same size. This hardware can also be configured with 32 processor stages which would further reduce the execution time of 0.025 s for such images.

The geometric filter was compared favorably ([34] - Appendix A) with the 3 x 3 median filter [21-29]. It was also compared favorably ([35, 36] - Appendicies B, C) with look-averaging [20, 32].

Exploration of filters in a class of non-linear filters failed to produce any that performed as well as the geometric filter.

2.2 THE GENERALIZED GEOMETRIC FILTER

One iteration of the geometric filter involves 32 basic operations, 16 of which increase pixel values and the other 16 decrease pixel values (see Appendix A). In the original version discussed above, a pixel value can be increased or decreased by at most one by each of these basic operations. This original version was developed for use on 8-bit SAR imagery.

A generalization of the geometric filter was developed for use on 16-bit SAR imagery. Because of the greater dynamic range, many iterations of the original version would be required to reduce the speckle significantly. The generalized version has an integer-valued control parameter n which allows for adjustment to the dynamic range of the image. Each of the 32 basic operations referred to above can increase or decrease a pixel value by at most n. With $n = 1$, the operation of the generalized version is identical to that of the original version. A program that computes one iteration of the generalized geometric filter is presented in Appendix D.

Experiments were performed to determine optimal settings for the control parameter. The maximum amount a pixel value can be changed in a single iteration is 16 n. For example, if there is a pixel in the image whose value is more than 16 n greater than the value of any other pixel in the image then its value will be reduced by 16 n. Thicker spikes will be reduced more slowly.

The speckle index (see Appendix A) was computed before and after running the filter with various settings of the control parameter. The extent to which the spatial information was preserved was judged subjectively.

By this somewhat ad hoc procedure it was found that the best results were achieved by halving the value of the control parameter on each successive iteration. It was also found that the maximum change in pixels values (= 16 n) for the first iteration should be about one quarter of the maximum pixel value in the image. This leads to the following method for setting the control parameter. On the first iteration the control parameter is set equal to n_1 where n_1 is the smallest power of two which is greater than or equal to maximum pixel value in the image divided by 64. The control parameter is then halved on each successive iteration. On the last iteration it has the value 1. This scheme results in $1 + \log_2 n_1$ iterations. If a 16-bit image is saturated then its maximum pixel value is $2^{16} - 1$ which results in 11 iterations.

Table 2-1 shows the speckle indices and maximum pixel values for the sequence of images obtained using this scheme on a 16-bit 512 x 512 X-band SAR magnitude image of an area in North Carolina near Rayleigh-Durham. (This imagery was made under USGS Contract No. 14-08-0001-21748). Table 2-1 also shows the reductions in the maximum pixel value for each iteration and the maximum possible reductions. The maximum pixel value in the original image is 1946 and 1946/64 = 30.4. Therefore the control parameter settings are 32, 16, 8, 4, 2 and 1 for the six iterations performed. (See Figures 2-1, 2-2 and 2-3.)

2.3 CONTRAST ENHANCEMENT ALGORITHM

Most digital display devices display 8-bit images, which is reasonable since the human vision system can perceive only about 8 bits' worth of grey-levels. In order to display a 16-bit image it must first be scaled down to 8-bits. The simplest method is to use a linear scaling which maps the maximum pixel value into 255 and the minimum into 0. However, if the image contains large sections with a relatively small dynamic range plus a few very bright points, this method will result in using very few quantization levels in large sections of the scaled-down image just to accommodate the few bright points. The generalized geometric filter produces images of this sort. By reducing the speckle it reduces the dynamic range in large sections of the image. On the other hand, it preserves small strong returns. Although the pixel values of these returns are reduced, they can still be fairly large.

TABLE 2-1
EFFECTS OF THE GENERALIZED GEOMETRIC FILTER

Iteration	Control Parameter n	Speckle Index	Maximum Pixel Value	Reduction in Max	Maximum Possible Reduction
0	N.A.	.475	1946	0	0
1	32	.068	1519	427	512
2	16	.039	1341	178	256
3	8	.029	1250	91	128
4	4	.024	1210	40	64
5	2	.0215	1190	20	32
6	1	.0202	1179	11	16

Note: The "0th" iteration is the original image.

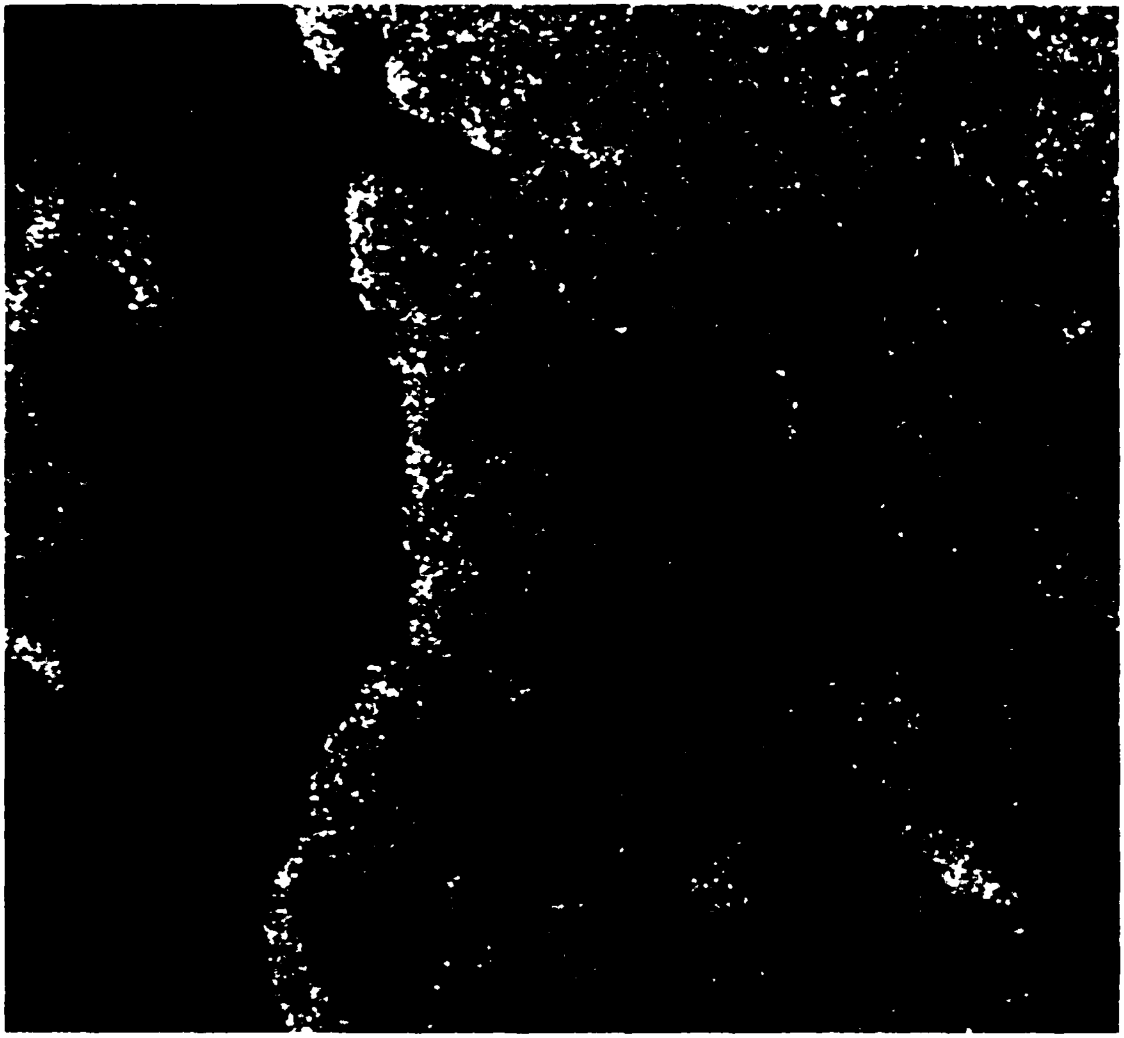

FIGURE 2-1. ORIGINAL IMAGE WITH SIMPLE GLOBAL LINEAR SCALING TO 8 BITS.

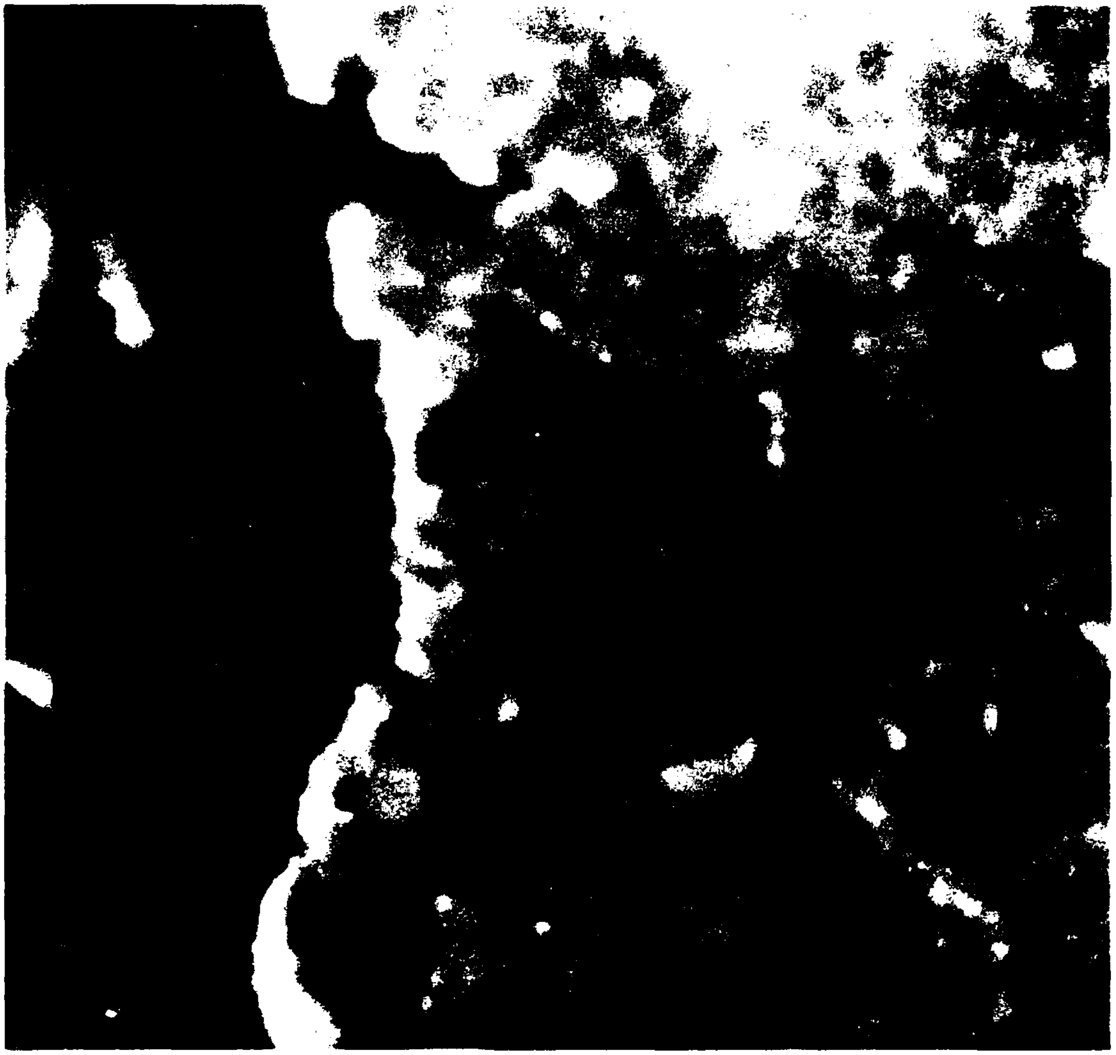

FIGURE 2-2. SPECKLE REDUCED IMAGE WITH SIMPLE GLOBAL LINEAR SCALING TO 8 BITS.

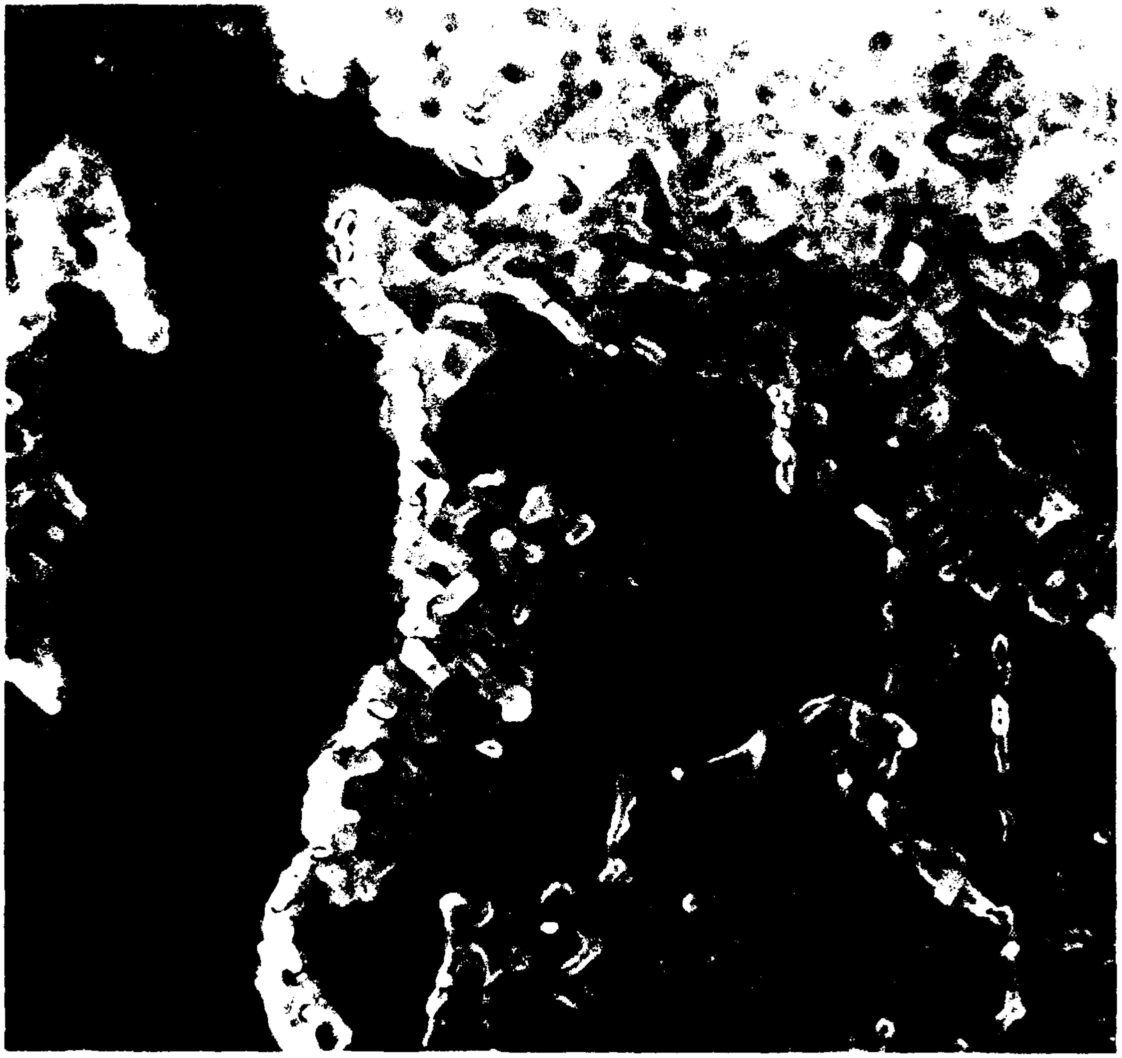

FIGURE 2-3. SPECKLE REDUCED IMAGE WITH CONTRAST ENHANCEMENT SCALING TO 8 BITS.

The contrast enhancement algorithm is basically a compromise between the global linear scaling defined above and an adaptive local linear scaling which uses local maxima and minima. If the adaptive local linear scaling is used by itself, all global contrast is lost and this global contrast can contain useful information. For example, a wooded area will be brighter than a pasture in the globally scaled image.

Let $f(m,n)$ represent the filtered image and let G be its global maximum and let H be its global minimum. Let $g_1(m,n)$ be the local maximum of f over a $N \times N$ square centered at (m,n), where N is an odd integer. (If the pixel (m,n) is close enough to an edge so that this square is not completely contained in the image, the local maximum is taken over the part of the square which is in the image.) Let $h_1(m,n)$ be similarly defined as the local minimum of the image f. In order to avoid the creation of artificial edges in the final image, the functions g_1 and h_1 are smoothed by convolving them with the function

$$\psi(m,n) = \begin{cases} c \operatorname{sinc}\left(\frac{\pi}{N+1}\right)m \ \operatorname{sinc}\left(\frac{\pi}{N+1}\right)n & \text{for } |m| \le N \text{ and } |n| \le N, \\ 0 \text{ otherwise,} \end{cases} \tag{1}$$

where c is chosen so that

$$\sum_{\substack{|m| \le N \\ |n| \le N}} \psi(m, n) = 1. \tag{2}$$

We define $g(m,n)$ as a convex combination of the smoothed local maximum and the global maximum G;

$$g(m,n) = \beta \sum_{\substack{|j| \le N \\ |k| \le N}} g_1(m + j, n + k)\psi(j, k) + (1 - \beta)G, \tag{3}$$

where β is an input parameter, $0 \leq \beta \leq 1$. (Appropriate modifications are made near edges.) Another function $h(m, n)$ is defined similarly as a convex combination (same β) of the smoothed local minimum and the global minimum H.

Finally, the contrast enhanced image is defined as

$$f_1(m, n) = \begin{cases} \dfrac{f(m, n) - h(m, n)}{g(m, n) - h(m, n)} \cdot 255 & \text{if } g(m, n) \neq h(m, n) , \\[2ex] \dfrac{f(m, n) - H}{G - H} \cdot 255 & \text{otherwise.} \end{cases}$$

The image in Figure 2-1 was obtained by simple global scaling ($\beta = 0$) of the original 16-bit image before running the generalized geometric filter on it. A 16-bit filter image was produced by running six iterations of the filter with n = 32, 16, 8, 4, 2 and 1, respectively. Figure 2-2 is the 8-bit image obtained by simple global linear scaling ($\beta = 0$) of the filtered image. Figure 2-3 is the 8-bit image obtained by running the contrast enhancement algorithm on the filtered image with N = 3 and $\beta = .95$.

3
PUBLICATIONS

The following papers were published during the performance of this contract.

1. T.R. Crimmins, "Geometric Filter for Speckle Reduction," Appl. Opt. 24(10), 1438-1443 (1985).
2. T.R. Crimmins, "Geometric Filter for Reducing Speckle," Proc. SPIE International Conf. on Speckle, 213-222 (August 1985).
3. T.R. Crimmins, "Geometric Filter for Reducing Speckle," Opt. Eng. 25(5), 651-654 (1986).

4
SCIENTIFIC PERSONNEL

The following scientific personnel participated in this project:

T.R. Crimmins

B.K. Eby

W.F. Pont

5
REFERENCES

1. A. Kozma, "Detectability of Objects in Speckle," Technical Report RR-CR-80-1, Research Directorate, U.S. Army Missile Laboratory, U.S. Army Missile Command, Redstone Arsenal, AL, October 1979.

2. C.R. Christensen, B.D. Guenther, J.S. Bennett, A. Jain, N. George, and A. Kozma, "Object Detectability in Speckle Noise," Internat. Conf. on Lasers, Orlando, FL, December 1978.

3. N. George, C.R. Christensen, J.S. Bennett, and B.D. Guenther, "Speckle Noise in Displays," J. Opt. Soc. Am., Vol. 66, p. 1282, 1976.

4. B.D. Guenther, N. George, C.R. Christensen, and J.S. Bennett, "Speckle Noise and Object Contrast," Photo. Sci. and Eng., Vol. 21, p. 192, 1977.

5. C.R. Christensen, N. George, B.D. Guenther, and J.S. Bennett, "Noise in Coherent Optical Systems: Minimum Detectable Object Contrast and Speckle Smoothing," Technical Report TR-RR-77-2, U.S. Army Missile Command, Redstone Arsenal, 1976.

6. V.N. Korwar and J.R. Pierce, "Detection of Gratings and Small Features in Speckle Imagery," Applied Optics, Vol. 20, No. 2, January 1981.

7. A. Kozma and C.R. Christensen, "Effects of Speckle on Resolution," J. Opt. Soc. Am., Vol. 66, No. 11, November 1976.

8. C.R. Christensen and A. Kozma, "The Effects of Speckle on Resolution of High Contrast and Continuous Tone Objects," Technical Report RR-77-2, Physical Sciences Directorate, U.S. Army Missile Research, Development and Engineering Laboratory, U.S. Army Missile Command, Redstone Arsenal, AL, December 1976.

9. H.H. Arsneault and G.V. April, "Information Content of Images Degraded by Speckle Noise," Opt. Eng. Vol. 25, No. 5, pp. 662-666, 1986.

10. V.S. Frost, J.A. Stiles, K.S. Shannugan, and J.C. Holtzman, "A Model for Radar Images and Its Application to Adaptive Digital Filtering of Multiplicative Noise," IEEE Trans. on Pattern Analysis and Machine Intelligence, Vol. PAMI-4, No. 2, March 1982.

11. A.K. Jain and C.R. Christensen, "Digital Processing of Images in Speckle Noise," SPIE, Vol. 243, Applications of Speckle Phenomena, 1980.

12. J.S. Lee, "Digital Image Enhancement and Noise Filtering by the Use of Local Statistics," IEEE Trans. Pattern Anal. Mach. Intelligence, PAMI-2, No. 2, 1980.

13. J.S. Lee, "Refined Filtering of Image Noise Using Local Statistics, Computer Graphics and Processing, Vol. 15, 1981.

14. J.S. Lee, "Speckle Analysis and Smoothing of Synthetic Aperture Radar Images," Computer Graphics and Image Processing, Vol 17, 1981.

15. T.S. McKechnie, "Speckle Reduction," in Laser Speckle and Related Phenomena, ed. by J.C. Dainty, Vol. 9 of Topics in Applied Physics, p. 123, Springer-Verlag, Berlin, 1975.

16. J.S. Lee, "A Simple Smoothing Algorithm for Synthetic Aperture Radar Images," IEEE Trans. Syst. Man., Cybern., Vol. 13, No. 1, January/February 1983.

17. J.S. Lim, "Image Restoration by Short Space Spectral Subtraction," IEEE Trans. Acoust., Speech, Signal Processing, Vol 26, p. 157, April 1978.

18. J.S. Lim and H. Nawab, "Techniques for Speckle Noise Removal," SPIE, Vol. 243, Applications of Speckle Phenomena, 1980.

19. E.G. Rawson, A.B. Nafarrate, R.E. Norton, and J.W. Goodman, "Speckle-Free Rear Projection Screen Using Two Close Screens in Slow Relative Motion," J. Opt. Soc. Am., Vol. 66, No. 11, p. 1290, 1976.

20. J.S. Zelenka, "Comparison of Continuous and Discrete Mixed-Integrator Processors," J. Opt. Soc. Am., Vol. 66, No. 11, p. 1295, 1976.

21. J.W. Tukey, "Nonlinear (Unsuperposable) Methods for Smoothing Data," in Cong. Rec., EASCON, p. 673, 1974.

22. J.W. Tukey, Exploratory Data Analysis, Reading, MA, Addison-Wesley, 1977.

23. T.S. Huang, G.J. Yang, and G.Y. Yang, "A Fast Two-Dimensional Medium Filtering Algorithm," IEEE Trans. Acoust., Speech, Signal Processing, Vol. ASSP-27, pp. 13-18, February 1979.

24. T.S. Huang and G.J. Yang, "Mexican Filters and Their Applications to Image Processing," School of Electrical Engineering, Purdue University, West Lafayette, IN, TR. EE 80-1, January 1980.

25. T.S. Huang, "Two-Dimensional Signal Processing -- II," in Topics in Applied Physics, Vol. 43, S.G. Tyan, Berlin, Springer-Verlag, 1981.

26. N.C. Gallagher, Jr. and G.L. Wise, "A Theoretical Analysis of the Properties of Median Filters," IEEE Trans. Acoust., Speech, Signal Processing, Vol. ASSP-29, No. 6, pp. 1136-1141, December 1981.

27. T.A. Nodes and N.C. Gallagher, Jr., "Median Filters: Some Modifications and Their Properties," IEEE Trans. Acoust., Speech, Signal Processing, Vol. ASSP-30, No. 5, October 1982.

28. G.R. Arce and N.C. Gallagher, Jr., "State Description for the Root-Signal Set of Median Filters," IEEE Trans. Acoust., Speech Signal Processing, Vol. ASP-30, No. 6, December 1982.

29. N.C. Gallagher, D.W. Sweeney, and C.R. Christensen, "Median Filtering of Speckle Noise," Technical Report RR-82-6, Research Directorate, U.S. Army Missile Laboratory, U.S. Army Missile Command, Redstone Arsenal, AL, 8 February 1982.

30. C.R. Christensen, A.K. Jain, and B.D. Guenther, Digital Filtering of Speckle Noise," J. Opt. soc. Am., Vol. 68, No. 10, p. 1376, 1978.

31. B.D. Guenther, C.R. Christensen, and Amil Jain, "Digital Processing of Speckle Images," Proc. IEEE on Pattern Recognition and Image Processing, Chicago, IL, May 1978.

32. L.J. Porcello, N.G. Massey, R.B. Innes, and J.M. Marks, "Speckle Reduction in Synthetic-Aperture Radars," J. Opt. Soc. Am., Vol. 66, No. 11, p. 1305, 1976.

33. J.S. Lee, "Speckle Suppression and Analysis for Synthetic Aperture Radar Images," Opt. Eng., Vol. 25, No. 5, pp. 636-643, 1986.

34. T.R. Crimmins, "Geometric Filter for Speckle Reduction," Appl. Opt., Vol. 24, No. 10, pp. 1438-1443, 1985.

35. T.R. Crimmins, "Geometric Filter for Reducting Speckle," Proc. SPIE International Conf. on Speckle, pp. 213-222, August 1985.

36. T.R. Crimmins, "Geometric Filter for Reducing Speckle," Opt. Eng., Vol. 25, No. 5, pp. 651-654, 1986.

37. J.W. Goodman, "Statistical Properties of Laser Speckle Patterns," in Laser Speckle and Related Phenomena, ed. by J.C. Dainty, Vol. 9 of Topics in Applied Physics, pp. 9-75, Springer-Verlag, Berlin, 1975.

38. J.C. Dainty, "Coherent Addition of a Uniform Beam to a Speckle Pattern," J. Opt. Soc. Am., Vol. 62, p. 595, 1972.

39. S.O. Rice, "Mathematical Analysis of Random Noise," in Selected Papers on Noise and Stochastic Processes, ed. by N. Wax, Dover Press, NY, 1954.

40. R.W. Larson, A. Dias, C. Liskow, and R. Majewski, "Digital Calibration Method for Synthetic Aperture Radar Systems," submitted to IEEE Trans. on Remote Sensing.

41. R.W. Larson, D.T. Politis, and J.L. Walker, "SAR Calibration: A Technology Review," Proceedings of the ESA SAR Calibration Workshop, Albach, Austria, December 1982.

42. "Amplitude Calibration Techniques Applied to the Environmental Research Institute of Michigan's Airborne Synthetic Aperture Radar System," ERIM, Radar and Optics Division, Technical Report AFAL-TR-74-239, Ann Arbor, MI, November 1974.

43. R.W. Larson and W. Carrara, "Radar Clutter Data Collection, Calibration, Digitization, and Analysis," ERIM, Radar and Optics Division, Technical Report AFAL-TR-79-1232, Ann Arbor, MI, December 1979.

44. R.W. Larson, R. Hamilton, F. Smith, and J. Haynes, "Calibration of Synthetic Apeture Radar," Proc. IGRSS, Washington, DC, June 1981.

45. D.T. Kuan, A.A. Sawchuk, and T.C. Strand, "Adaptive Restoration of Images with Speckle," SPIE, Vol. 259, Applications of Digital Image Processing IV, 1982.

46. R.M. Lougheed, "A High Speed Recirculating Neighborhood Processing Architecture," SPIE, Vol. 534, Architectures and Algorithms for Digital Image Processing II, 1985.

APPENDIX A

"GEOMETRIC FILTER FOR SPECKLE REDUCTION"

T. R. Crimmins

Published in Applied Optics
Vol. 24, No. 10, 1438-1443 (15 May 1985).

Reprinted from Applied Optics, Vol. 24, page 1438, May 15, 1985

Geometric filter for speckle reduction

Thomas R. Crimmins

An algorithm is described which reduces speckle noise in images. It is a nonlinear algorithm based on geometric concepts. Tests were performed on synthetic aperture radar images which show that it compares favorably with a 3 × 3 median filter.

I. Introduction and Results

It is desirable to reduce speckle noise in synthetic aperture radar images both to assist radar image interpreters and to preprocess images for automatic recognition algorithms on computers. The goal is to smooth the speckle but at the same time preserve features of interest such as edges, strong returns, etc.

A nonlinear algorithm based on geometric concepts was developed to accomplish this. It is an iterative algorithm and usually about ten iterations seems to be optimal although just two or three iterations will reduce the speckle significantly (see Table I). It was programmed on a DeAnza IP5000 digital video processor using a VAX 11/780 as a host system. Running time was 14 sec/iteration.

Figure 1 is a synthetic aperture radar image of Willow Run Airport in southeastern Michigan. It is an X-band strip map image which was digitally processed on the ERIM digital processor. The polarization of both transmitter and receiver was horizontal. The resolution, measured as the half-power width of the impulse response function, is 6 m. Figure 2(a) is a subimage of Fig. 1. The pixel spacing in Fig. 2(a) is 3 m and the image is 512 × 512 pixels.

Figure 2(b) shows the result of four iterations of the geometric filter, and Fig. 2(c) shows the result of ten iterations. For comparison, Fig. 2(d) shows the result of applying the 3 × 3 median filter[1–8] until this image was obtained which is of period 2 under the median filter. That is, one application of the median filter to this image will change it (very slightly) but it is invariant under two applications of the median filter. (It is interesting to note that this means that this image, and hence the original image, have no median roots. This contrasts with the 1-D case in which median roots always exist.[6]) The 3 × 3 median filter replaces each pixel value with the median of the nine pixel values in its 3 × 3 neighborhood window. Figures 3(a), (b), and (c) are shaded and shadowed versions of Figs. 2(a), (c), and (d), respectively, considered as 2-D surfaces in 3-D space.

Because speckle noise is multiplicative, the ratio of its deviation to its mean seems to be a reasonable measure of the amount of speckle noise present (see Ref. 9, p. 25).

Let $p(m,n), 1 \le m,n \le N$, be the pixel values. For $2 \le m,n \le N - 1$, the local deviation is defined as

$$\sigma(m,n) = \max_{\substack{-1 \le i \le 1 \\ -1 \le j \le 1}} p(m+i,n+j) - \min_{\substack{-1 \le i \le 1 \\ -1 \le j \le 1}} p(m+i,n+j) \tag{1}$$

(This, of course, is not the true deviation, but it is easy to compute and we believe it should be good enough for our present purpose.) The local mean is defined as

$$\mu(m,n) = \frac{1}{9} \sum_{i,j=-1}^{1} p(m+i,n+j) \tag{2}$$

Finally, the speckle index is defined as

$$\frac{1}{(N-2)^2} \sum_{m,n=2}^{N-1} \frac{\sigma(m,n)}{\mu(m,n)} . \tag{3}$$

Table I gives the speckle index for the original image for various numbers of iterations of the geometric filter and for the median root. Of course the goal here is to reduce the speckle index as much as possible while still preserving the spatial information in the image. The images in Figs. 2 and 3 indicate how well the spatial information was preserved. Thus the speckle index must be considered together with the corresponding images in order to determine how well a given filter performs.

The geometric filter utilizes a technique which has a history starting with a problem which has nothing to do with speckle reduction. The original problem was

The author is with Environmental Research Institute of Michigan, Radar Division, P.O. Box 8618, Ann Arbor, Michigan 48107.

Received 23 January 1985.

0003-6935/85/101438-06$02.00/0.

Table I. Speckle Indices

Image	Speckle index
Original image	1.400
Four iterations of geometric filter	0.380
Ten iterations of geometric filter	0.182
Period 2 median root	0.333

Fig. 1. Radar image of Willow Run Airport. The boxed section appears in Fig. 2(a).

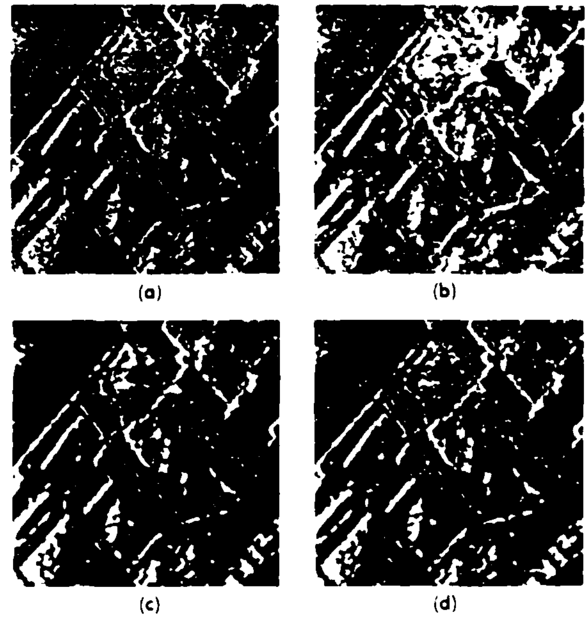

Fig. 2. (a) Original image. (b) Four iterations of geometric filter. (c) Ten iterations of geometric filter. (d) Period 2 median root of original image.

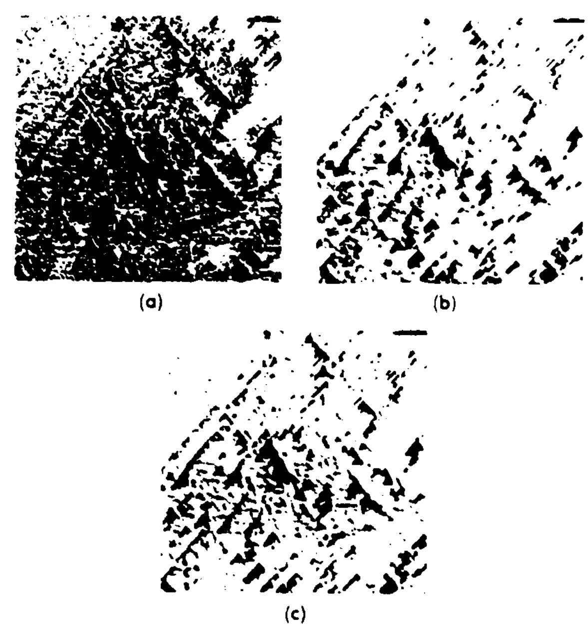

Fig. 3. (a) Shaded and shadowed version of original image. (b) Shaded and shadowed version of ten iterations of geometric filter. (c) Shaded and shadowed version of period 2 median root of original image.

to generate approximations of the convex hulls of maximal connected subsets of the foreground of a binary image. (A binary image is an image whose pixels have only the values 0 and 1. The foreground is the set of pixels with value 1.) The motivation for this was enhancement of medical imagery.

II. The 8-Hull Algorithm

The convex hull of a set is the intersection of all the half-planes containing it. An approximation to this, called the 8-hull, is defined as the intersection of only those half-planes which contain the set and whose edges are either horizontal or vertical or lie in either of the 45° diagonal directions. The 8-hull of a set has, at most, eight sides.

P. Lambeck wrote an iterative algorithm (unpublished) which generates the 8-hull of a set. It works as follows. At each step of the iteration, the value of a pixel is changed from a 0 to a 1 if its neighboring pixels have ones arranged in any one of the configurations shown in Fig. 4. The blank squares can be either zeros or ones. If enough iterations of this step are performed, eventually the 8-hull of the given set will be generated and it will be invariant under further iterations. An example of the 8-hull of a set being formed is shown in Figs. 5. The black squares represent ones and the white squares represent zeros.

III. Complementary Hulling Algorithm

Next, J. Gleason developed an iterative algorithm (unpublished) for smoothing the ragged edges of binary images of vehicles obtained by slicing gray-level radar images. We will refer to this algorithm as the complementary hulling algorithm. One step of the iteration

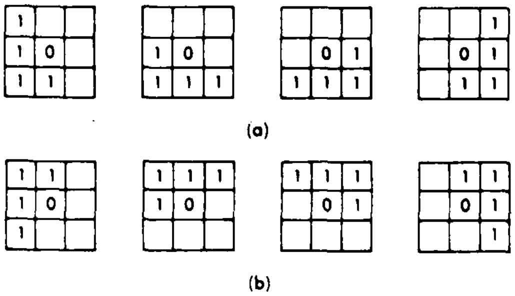

Fig. 4. Patterns used by the 8-hull algorithm.

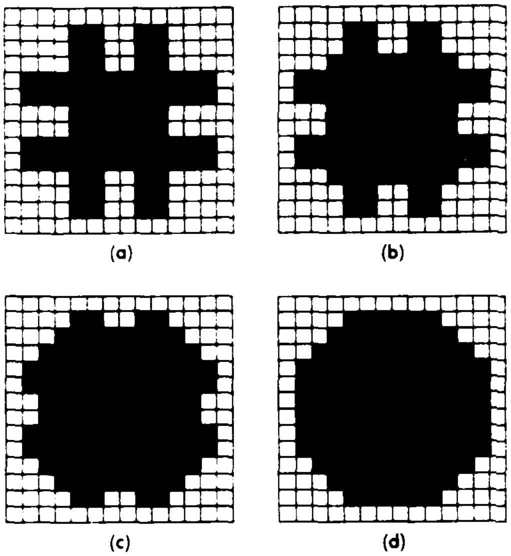

Fig. 5. (a) Original set. (b) One iteration of 8-hull algorithm. (c) Two iterations. (d) Three iterations. This is invariant under further iterations.

consists of the following. First, one step of the 8-hull algorithm described above is applied to the set and then one step of the 8-hull algorithm is applied to its complement. In other words, one step of the 8-hull algorithm is applied, then zeros and ones are interchanged, then another step of the 8-hull algorithm is applied, and finally, zeros and ones are interchanged again. This has the effect of gradually reducing the maximum curvature of the boundary of the set. (Curvature is the inverse of the radius of curvature.) More precisely, with a few exceptions, the boundary of a set invariant under this algorithm can turn a maximum of 45° at any vertex. The only known exceptions to this rule are the boundary segments shown in Fig. 6 and their 90° rotations.

Figure 7 shows a set at various stages of the iteration process. The ninth iteration is invariant under further iterations. Figure 8 shows the effect of this algorithm on a set with a tower three pixels wide protruding from the top. If one imagines going up the left side of this tower and then down the right side, a sharp U-turn must be made at the top. This U-turn has too high a curvature to be permissible. Hence, the algorithm reduces it until the curvature is sufficiently small. A tower seven pixels wide is shown in Fig. 9. Here the U-turn

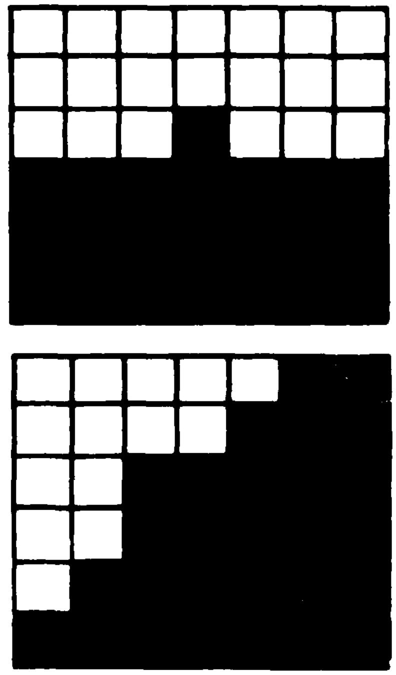

Fig. 6. Allowable 90° turns in the boundary. These are exceptions to the rule.

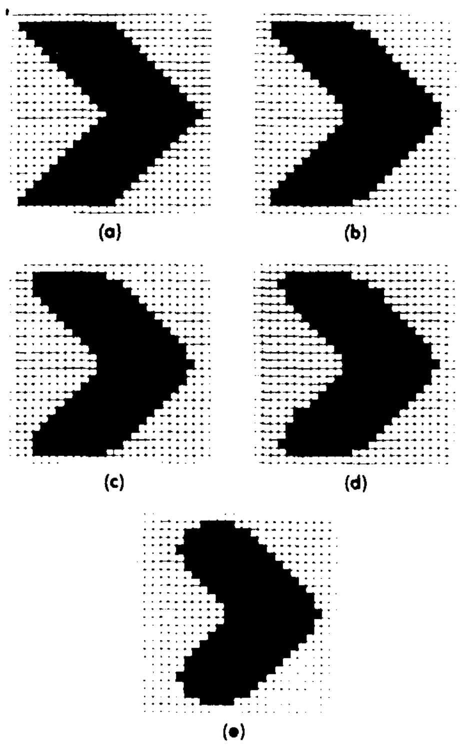

Fig. 7. (a) Original set. (b) One iteration of complementary hulling algorithm. (c) Two iterations. (d) Three iterations. (e) Nine iterations. This is invariant under further iterations.

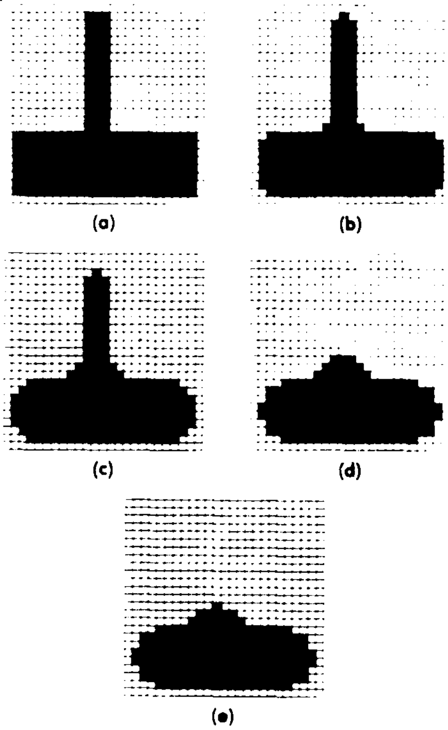

Fig. 8. (a) Original set. (b) One iteration of complementary hulling algorithm. (c) Two iterations. (d) Fourteen iterations. (e) Fifteen iterations. This is invariant under further iterations.

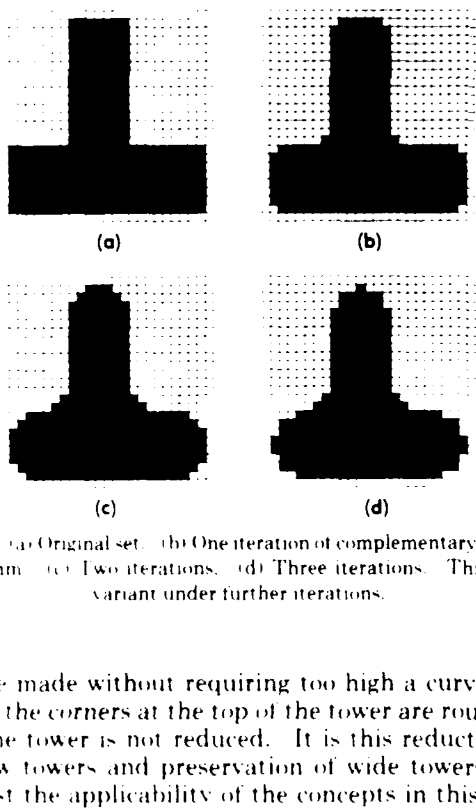

Fig. 9. (a) Original set. (b) One iteration of complementary hulling algorithm. (c) Two iterations. (d) Three iterations. This is invariant under further iterations.

can be made without requiring too high a curvature. Thus, the corners at the top of the tower are rounded, but the tower is not reduced. It is this reduction of narrow towers and preservation of wide towers that suggest the applicability of the concepts in this algorithm to speckle reduction.

IV. Geometric Filter

A. How It Works

The geometric filter uses this complementary hulling technique in the following way. First, picture the gray-level (pixel values between 0 and 255 inclusive) radar image lying horizontally with its sides running in the north–south (N–S) direction and its top and bottom running in the east–west (E–W) direction. We now construct a gray-level surface above the image such that its height above any pixel is proportional to the value of that pixel. Next, this surface is sliced by all vertical planes which contain a line of pixels running in the E–W direction. A discrete grid is defined on each of these vertical planes composed of vertical lines which pass through pixels in the image and horizontal lines at heights representing the integers between 0 and 255 inclusive. The points in this vertical grid will be referred to as vertical pixels. Then the intersection of any one of the vertical planes with the gray-level surface is a curve composed of vertical pixels in the vertical grid [Fig. 10(a)]. Now consider the umbra of this curve. The umbra consists of all vertical pixels in the vertical grid on or below the curve [Fig. 10(b)]. If we assign the value 1 to all vertical pixels in the umbra and the value 0 to all other vertical pixels in the vertical grid, the vertical grid can be considered as a binary image. (Note: It is not necessary for the algorithm to actually construct this binary image. We construct it here only for pedagogic purposes.) Now one iterative step of the complementary hulling algorithm is applied to the umbra, which is the foreground of the vertical binary image just constructed. Recall that the first half of an iterative step of the complementary hulling algorithm consists of one step of the 8-hull algorithm. Since we are only concerned with the line forming the top boundary of the umbra, only four of the eight configurations shown in Fig. 4 need be used. These four are shown in Fig. 4(a). Similarly, in the second half of an iterative step of the complementary hulling algorithm, when one iterative step of the 8-hull algorithm is applied to the complement [Fig. 10(c)], only the line forming the bottom boundary of the complement is of interest and hence only the four configurations shown in Fig. 4(b) are used. As before, the complementary hulling algorithm step is completed by complementing back. This procedure is performed on all E–W vertical grids simultaneously and the resulting gray-level image replaces the original gray-level image. Now the same procedure is repeated in the SW–NE direction, then in the S–N direction, and finally in the SE–NW direction. This completes one iterative step of the geometric filter.

One change has been made in the algorithm described above to speed the speckle reduction. It has to do with the application of an iterative step of the 8-hull algorithm to the umbra of a vertical slice as described above. Instead of changing a 0 to a 1 if any of the four neighborhood configurations in Fig. 4(a) is present, these four configurations are used separately and consecutively. That is, first a 0 is changed to a 1 if the first of these four configurations is present. Then the resulting image

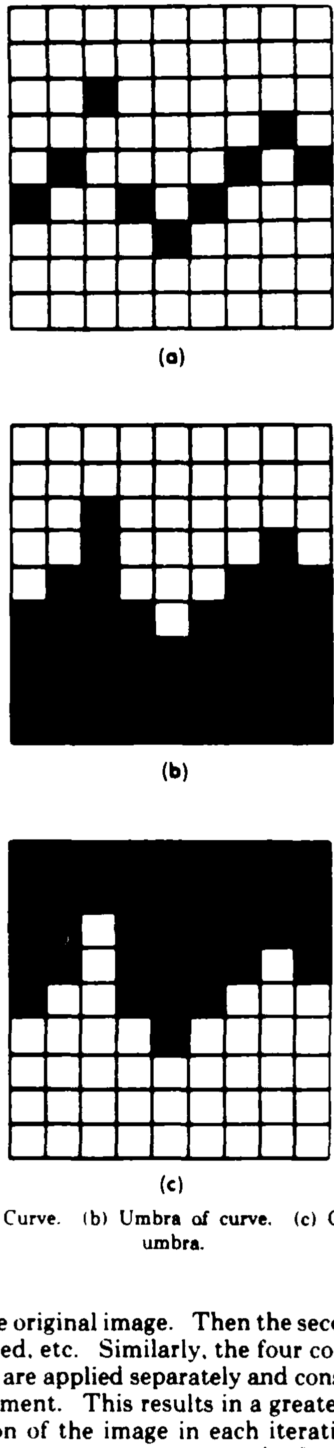

(a)

(b)

(c)

Fig. 10. (a) Curve. (b) Umbra of curve. (c) Complement of umbra.

Table II. Reduction Rates for Square Towers

Tower size	Reduction of maximum/iteration; number of vertical pixels, i.e., units of intensity
1 × 1	16
2 × 2	9
3 × 3	6
4 × 4	5
5 × 5	4
6 × 6	3
7 × 7	2
8 × 8	2

Table III. Reduction Rates for Walls

Wall width	Reduction of maximum/iteration; number of vertical pixels, i.e., units of intensity
1	12
2	6
3	3
4	3
5	2
6	1.5
7	0

replaces the original image. Then the second configuration is used, etc. Similarly, the four configurations in Fig. 4(b) are applied separately and consecutively to the complement. This results in a greater amount of modification of the image in each iterative step and hence fewer iterations are required. It also causes a greater difference between the reduction rates for wide and narrow features (see next subsection).

B. Why It Works

Speckle has a wormy appearance. Considering the image as a curved 2-D surface in 3-D space (as described above), speckle appears as narrow winding walls and valleys. A strong target return appears as a wide tall tower. The entire body of the target appears as an even wider high plateau, although it is not as high as the tower representing a strong target return. The geometric filter, through iterative repetition, gradually tears down the narrow walls and fills up the narrow valleys. It also tears down towers and high plateaus, which we want to preserve. However, it reduces narrow walls and valleys faster than it reduces wide towers, and the even wider plateaus are reduced even more slowly than the wide towers. In general, the wider any landscape feature (valleys, holes, depressions, walls, towers, plateaus) is, the more slowly it is reduced. Thus, only a few iterations are required to reduce the narrow speckle walls and valleys and these few iterations have very little effect on wide high towers (hence, strong target returns are preserved) or on the even wider plateaus (hence, target shape is preserved).

Since the algorithm works on both the umbra of the image surface and its complement, it is essentially symmetric with respect to up and down. Thus, filling up valleys is essentially equivalent to tearing down walls. Tables II and III show the rates at which the height (maximum) of walls and square towers is being reduced. In the case of the wider towers and walls, the reduction rate may be less for the first few iterations. The tables show the rates established after these first few iterations. However, this lag becomes important for wider towers. For example, the maximum of a 14 × 14 tower is not reduced at all until the fifth iteration.

One more thing should be mentioned here. Sometimes the tower representing a strong target return is almost as narrow as the speckle walls and valleys. However, such a tower is usually much higher than the speckle walls are high or valleys deep. Thus, although it may be reduced at as fast a rate as the speckle walls and valleys, the walls and valleys will still be reduced before the tower is completely torn down and hence the strong target return will still be preserved, although it will be dimmer than in the original image.

This work supported in part by the Army Research Office, Physics division, under contract DAAG29-84-K-0204.

References

1. J. W. Tukey, "Nonlinear (Nonsuperposable) Methods for Smoothing Data," in Congressional Record 1974, EASCON, p. 673.
2. J. W. Tukey, *Exploratory Data Analysis* (Addison-Wesley, Reading, Mass., 1977).
3. T. S. Huang, G. J. Yang, and G. Y. Yang, "A Fast Two-Dimensional Medium Filtering Algorithm," IEEE Trans. Acoust. Speech Signal Process. **ASSP-27**, 13 (1979).
4. T. S. Huang and G. J. Yang, "Median Filters and Their Applications to Image Processing," School of Electrical Engineering, Purdue U., West Lafayette, Ind., TR. EE 80-1 (Jan. 1980).
5. S. G. Tyan, "Median Filtering: Deterministic Properties," in *Two-Dimensional Digital Signal Processing. Vol. 2: Transforms and Median Filters*, T. S. Huang, Ed. (Springer, Berlin, 1981).
6. N. C. Gallagher, Jr., and G. L. Wise, "A Theoretical Analysis of the Properties of Median Filters," IEEE Trans. Acoust. Speech Signal Process. **ASSP-29**, 1136 (1981).
7. T. A. Nodes and N. C. Gallagher, Jr., "Median Filters: Some Modifications and Their Properties," IEEE Trans. Acoust. Speech Signal Process. **ASSP-30**, 739 (1982).
8. G. R. Arce and N. C. Gallagher, Jr., "State Description for the Root-Signal Set of Median Filters," IEEE Trans. Acoust. Speech Signal Process. **ASSP-30**, 894 (1982).
9. J. W. Goodman, "Statistical Properties of Laser Speckle Patterns," in *Laser Speckle and Related Phenomena*, J. C. Dainty, Ed. (Springer, Berlin, 1975), pp. 9–75.

APPENDIX B

"GEOMETRIC FILTER FOR REDUCING SPECKLE"

T. R. Crimmins

Presented at the SPIE International Conference on Speckle in San Diego, California, August 20-23, 1985, and published in the Proceedings of that conference, pp. 213-222.

Geometric filter for reducing speckle

Thomas R. Crimmins

Radar Division, Environmental Research Institute of Michigan
P.O. Box 8618, Ann Arbor, MI 48107

Abstract

A non-linear speckle filter based on geometric concepts is defined and an example of its effectiveness on synthetic aperture radar imagery is shown. A comparison with look-averaging is made using artificial imagery with synthetic speckle.

Introduction

The presence of speckle in imagery produced with coherent illumination reduces the detectability of objects in the images[1 - 8]. It also reduces the effectiveness of some computer algorithms (e.g., edge detection) designed for automatic image analysis.

The geometric filter was designed to reduce speckle in synthetic aperture radar (SAR) imagery while preserving the spatial information in the image such as edges, strong returns, etc. It is an iterative non-linear algorithm. Usually from 4 to 10 iterations are used. The algorithm was implemented on a DeAnza IP 5500 digital video processor using a VAX 11/780 as a host system. Running time is about 14 seconds per iteration for 512 x 512 pixel images.

Definition of the geometric filter

The geometric filter algorithm is based on applying a single iteration of an iterative convex hulling algorithm alternately to the image and to its complement (negative of the image). For details of the geometric derivation and an intuitive explanation of the program below, see Crimmins[9].

It is essentially a one-dimensional algorithm which is applied successively in four different directions in the two-dimensional image; horizontal, vertical, and the two diagonal directions. The algorithm is defined as follows. The image is a function $f(m, n)$ where $1 \leq m \leq M$, $1 \leq n \leq N$ and the values of f are integers between 0 and 255. A border of zeros is added to the image so that $f(m, n)$ is defined for $0 \leq m \leq M + 1$ and $0 \leq n \leq N + 1$. An auxiliary image $g(m, n)$ is used which is initially set equal to zero on the same extended domain. The following program computes one iteration of the geometric filter.

1. $a \leftarrow 1,\ b \leftarrow 0,\ c \leftarrow 3,\ d \leftarrow 1$.
2. $g(m, n) \leftarrow \max \{ f(m, n),\ \min [f(m-a, n-b)-1, f(m, n) + 1]\}$, for $1 \leq m \leq M$, $1 \leq n \leq N$.
3. $f(m, n) \leftarrow \max \{ g(m, n),\ \min [g(m - a, n - b), g(m, n) + 1, g(m + a, n + b) + 1]\}$,
   for $1 \leq m \leq M$, $1 \leq n \leq N$.
4. If $d = 1$; $a \leftarrow -a$, $b \leftarrow -b$, $d \leftarrow 0$, go to 2. If $d = 0$; $d \leftarrow 1$, go to 5.
5. $g(m, n) \leftarrow \min \{ f(m, n),\ \max [f(m - a, n - b) + 1, f(m, n) - 1]\}$,
   for $1 \leq m \leq M$, $1 \leq n \leq N$.
6. $f(m, n) \leftarrow \min \{ g(m,n),\ \max [g(m - a, n - b), g(m, n) - 1, g(m + a, n + b) - 1]\}$,
   for $1 \leq m \leq M$, $1 \leq n \leq N$.
7. If $d = 1$; $a \leftarrow -a$, $b \leftarrow -b$, $d \leftarrow 0$, go to 5.
   If $d = 0$, $d \leftarrow 1$, go to 8.
8. If $c = 3$; $a \leftarrow 0$, $b \leftarrow 1$, $c \leftarrow 2$, go to 2.
   If $c = 2$; $a \leftarrow 1$, $b \leftarrow 1$, $c \leftarrow 1$, go to 2.
   If $c = 1$; $a \leftarrow 1$, $b \leftarrow -1$, $c \leftarrow 0$, go to 2.
   If $c = 0$; stop.

Example

Figure 1 is a SAR image of an airport in Windsor, Ontario. It was made by the STAR-1 airborne SAR system designed and developed by the Environmental Research Institute of Michigan (ERIM). The resolution is 6 m x 6 m and the pixel spacing is 8.4 m. Figure 2 shows the result of applying 5 iterations of the geometric filter.

Note that small strong returns retain their sharp edges in the filtered image. Also medium contrast edges retain their sharpness and low contrast edges are still visible in the filtered image. Figure 3 shows 3-D plots of the boxed small strong return in the original and filtered images. Figure 4 shows similar 3-D plots for the boxed medium contrast edge.

In order to measure the "amount" of speckle reduction, we define a speckle index as follows. In view of the multiplicative nature of speckle noise (Goodman[10], p. 25), the ratio of its deviation to its mean seems to be a reasonable measure of the amount of speckle noise present. For $1 \le m \le M$ and $1 \le n \le N$, we define an approximation to the local deviation by

$$\sigma(m, n) = \max_{-1 \le a, b \le 1} f(m + a, n + b) - \min_{-1 \le a, b \le 1} f(m + a, n + b). \tag{1}$$

The local mean is defined as

$$\mu(m, n) = \frac{1}{9} \sum_{a,b=-1}^{1} f(m + a, n + b) \tag{2}$$

The speckle index is then defined by,

$$\text{speckle index} \equiv \frac{1}{MN} \sum_{m=1}^{M} \sum_{n=1}^{N} \frac{\sigma(m, n)}{\mu(m, n)} \tag{3}$$

The speckle index for the original image shown in Figure 1 is 1.05. The filtered image shown in Figure 2 has a speckle index of 0.36.

Synthetic imagery

In order to create an image with synthetic speckle, we begin by choosing a real-valued image, $r(m, n)$, containing some patterns of interest. A random phase image, $\phi(m, n)$, is generated where, for each point (m, n), $\phi(m, n)$ is an independent sample from the uniform distribution over the interval from 0 to 2π. We then define a synthetic complex reflectivity function by

$$g(m, n) = r(m, n) \exp [j \phi(m, n)] \tag{4}$$

where $j = (-1)^{1/2}$. An impulse response function is defined by

$$k(m, n) = \begin{cases} (\operatorname{sinc} \frac{\pi}{2} m)(\operatorname{sinc} \frac{\pi}{2} n) & \text{for } |m|, |n| \le 2, \\ 0 & \text{otherwise.} \end{cases} \tag{5}$$

The synthetic complex radar image is defined by $h = k * g$ where $*$ denotes convolution. Finally, the synthetic detected image is defined by $f(m, n) = |h(m, n)|$. This detected image is then modified by a two step process which is used at ERIM on real radar imagery to reduce 16-bit signed data to 8-bit unsigned data for display on a CRT. It consists of a linear scaling followed by a non-linear mapping.

The image $r(m, n)$ used to create the synthetic image in Figure 5a has a background level of 12. It has five rows of squares of sizes 32 x 32, 16 x 16, 8 x 8, 4 x 4 and 2 x 2 pixels. The pixel values of the squares, going from left to right, are 170, 130, 90 and 50. The two large gratings consist of bright and dark stripes of dimension 64 x 6 pixels. The bright stripes have a pixel value of 170 in the first grating and 90 in the second. The dark stripes are at the background level of 12. The stripes in the four smaller gratings have dimension 32 x 4. The bright stripes have pixel values 170, 130, 90 and 50, and the dark stripes are at the background level of 12.

Comparison with look-averaging

Look averaging, the noncoherent addition of multiple images, is a commonly used technique to reduce speckle noise in SAR imagery and is an obvious reference for comparing the effectiveness of the geometric filter. In order to make a fair comparison between the geometric filter and look-averaging, the same information was used for both methods.

Look-averaging was carried out as follows. The Fourier transform of the complex image (= $h(m, n)$ - see the preceeding section) was taken and its square domain was divided into four smaller squares. Each of these four parts of the Fourier transform were then inverse-transformed to obtain four complex looks. The detected looks were obtained by computing the magnitude of the complex looks. Finally, the average of these four detected looks was computed.

The result of this look-averaging process is the image in Figure 5b. The result of five iterations of the geometric filter applied to the original image is in Figure 5c. The speckle indices for these three images are given in Table 1.

Table 1. Speckle Indices

Image	Speckle Index
Original	0.524
Look-average	0.223
Geometric filter	0.065

Figure 6 shows 3-D plots of the boxed square. Figure 7 shows 2-D plots of a slice through the same square and Figure 8 shows 2-D plots of a slice across part of one of the gratings.

It appears from the above that, at least in this case, the geometric filter outperforms look-averaging. Thus, it could be used either to produce higher quality imagery or perhaps to produce imagery of the same quality at a lower cost from less data.

Summary

The geometric filter has become a standard tool at ERIM for use in processing SAR imagery. It has been found to be useful in preparing imagery both for human inspection and for computer algorithms such as edge detection. It reduces speckle effectively while at the same time preserving the spatial information in the image such as edges, strong returns, etc. This filter appears to outperform the commonly used look-averaging method for reducing speckle.

Acknowledgments

This work was supported by the Army Research Office, Physics Division, under contract DAAG 29-84-K-0204.

References

1. A. Kozma, "Detectability of Objects in Speckle," Technical Report RR-CR-80-1, Research Directorate, U.S. Army Missile Laboratory, U.S. Army Missile Command, Redstone Arsenal, AL, October 1979.
2. C.R. Christensen, B.D. Guenther, J.S. Bennett, A. Jain, N. George, and A. Kozma, "Object Detectability in Speckle Noise," Internat. Conf. on Lasers, Orlando, FL, December 1978.
3. N. George, C.R. Christensen, J.S. Bennett, and B.D. Guenther, "Speckle Noise in Displays," J. Opt. Soc. Am., Vol. 66, p. 1282, 1976.
4. B.D. Guenther, N. George, C.R. Christensen, and J.S. Bennett, "Speckle Noise and Object Contrast," Photo. Sci. and Eng., Vol. 21, p. 192, 1977.
5. C.R. Christensen, N. George, B.D. Guenther, and J.S. Bennett, "Noise in Coherent Optical Systems: Minimum Detectable Object Contrast and Speckle Smoothing," Technical Report TR-RR-77-2, U.S. Army Missile command, Redstone Arsenal, 1976.
6. V.N. Korwar and J.R. Pierce, "Detection of Gratings and Small Features in Speckle Imagery," Applied Optics, Vol. 20, No. 2, January 1981.
7. A. Kozma and C.R. Christensen, "Effects of Speckle on Resolution," J. Opt. Soc. Am., Vol. 66, No. 11, November 1976.
8. C.R. Christensen and A. Kozma, "The Effects of Speckle on Resolution of High Contrast and Continuous Tone Objects," Technical Report RR-77-2, Physical Sciences Directorate, U.S. Army Missile Research, Development and Engineering Laboratory, U.S. Army Missile Command, Redstone Arsenal, AL, 148 December 1976.
9. T.R. Crimmins, "Geometric Filter for Speckle Reduction," Applied Optics, Vol. 24, No. 10, 15 May 1985.
10. J.W. Goodman, "Statistical Properties of Laser Speckle Patterns," in Laser Speckle and Related Phenomena, J.C. Dainty, Ed. (Springer, Berlin, 1975), pp. 9-75.

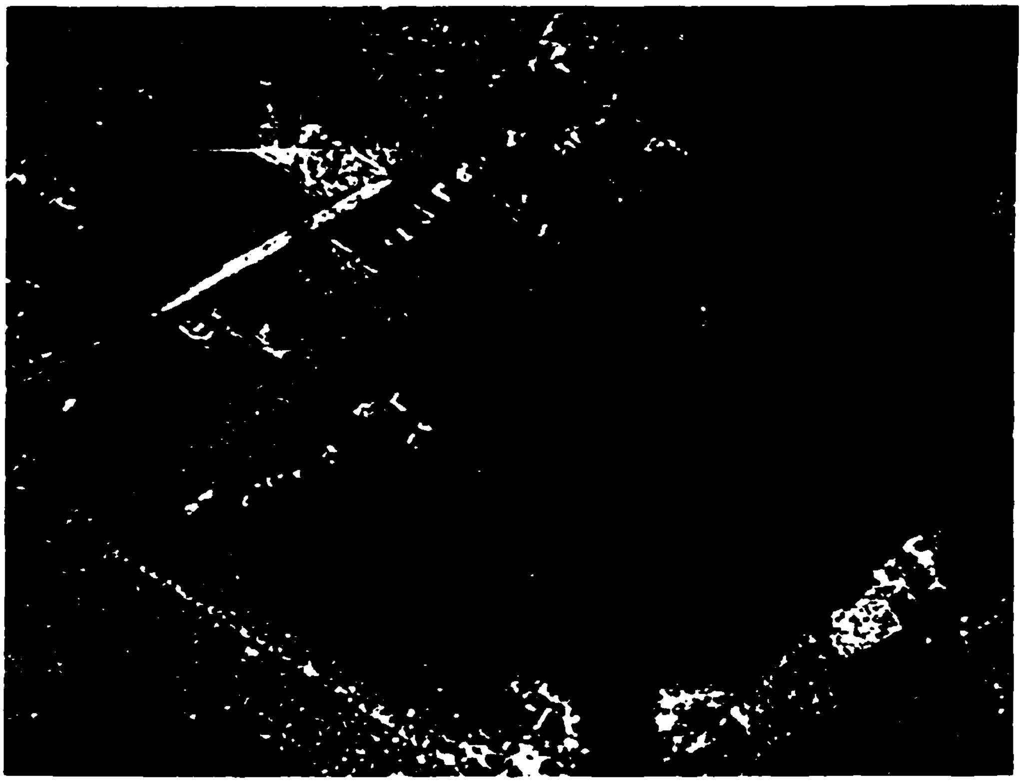

Figure 1. Original SAR image.

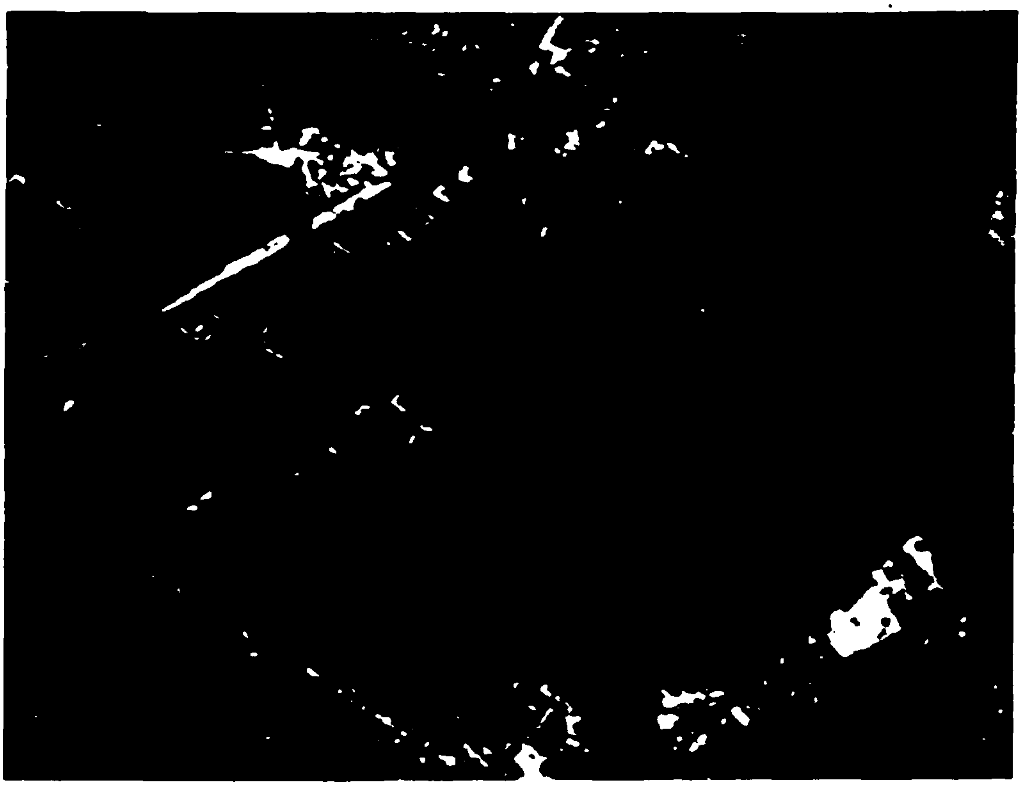

Figure 2. Result of 5 iterations of geometric filter.

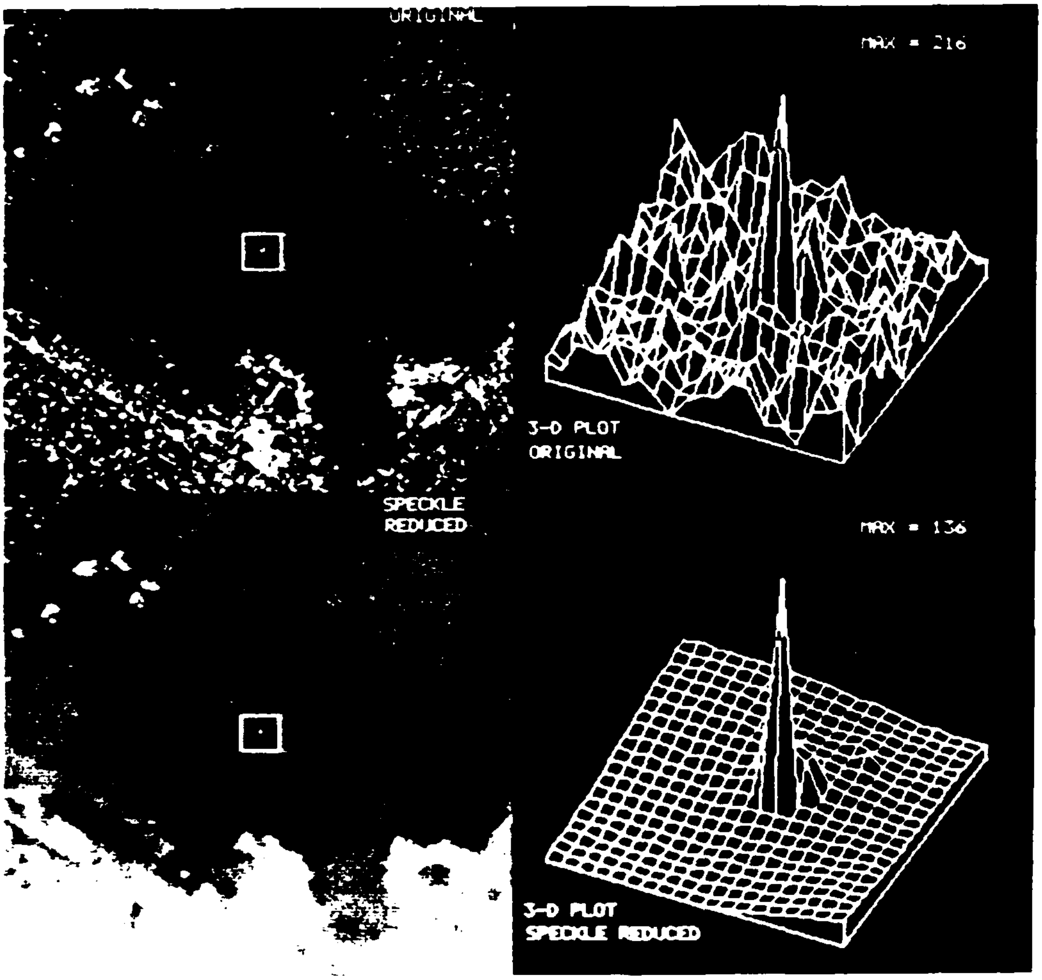

Figure 3. Three-dimensional plots of a small strong return.

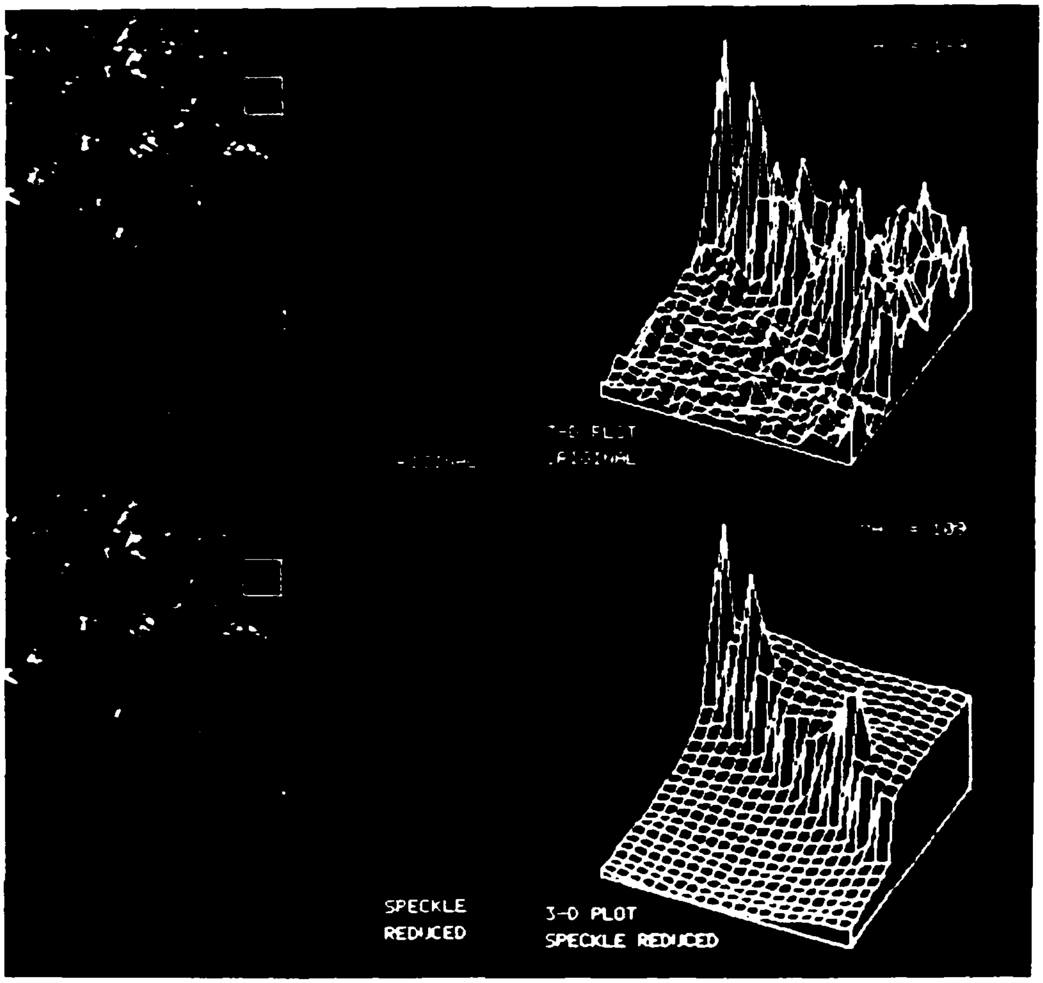

Figure 4. Three-dimensional plots of a medium contrast site.

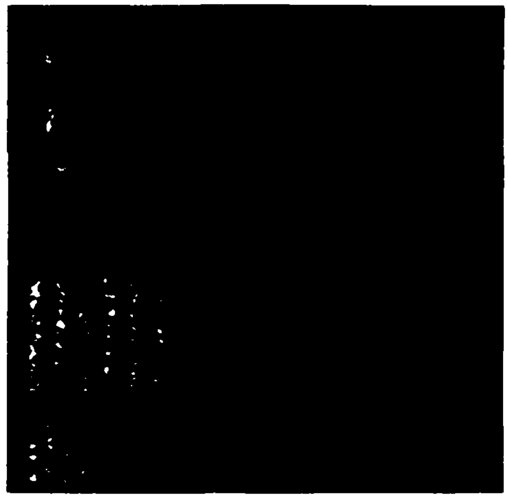

(a)

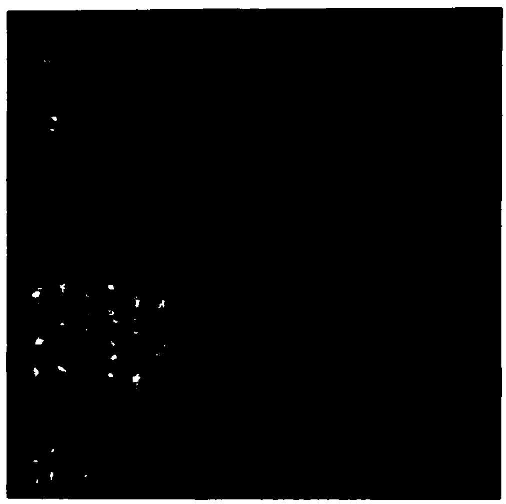

(b)

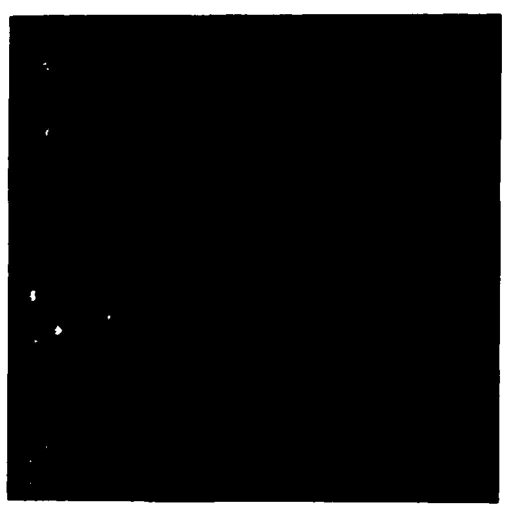

(c)

Figure 5. (a) Original image with synthetic speckle. (b) Average of four looks. (c) Result of five iterations of geometric filter.

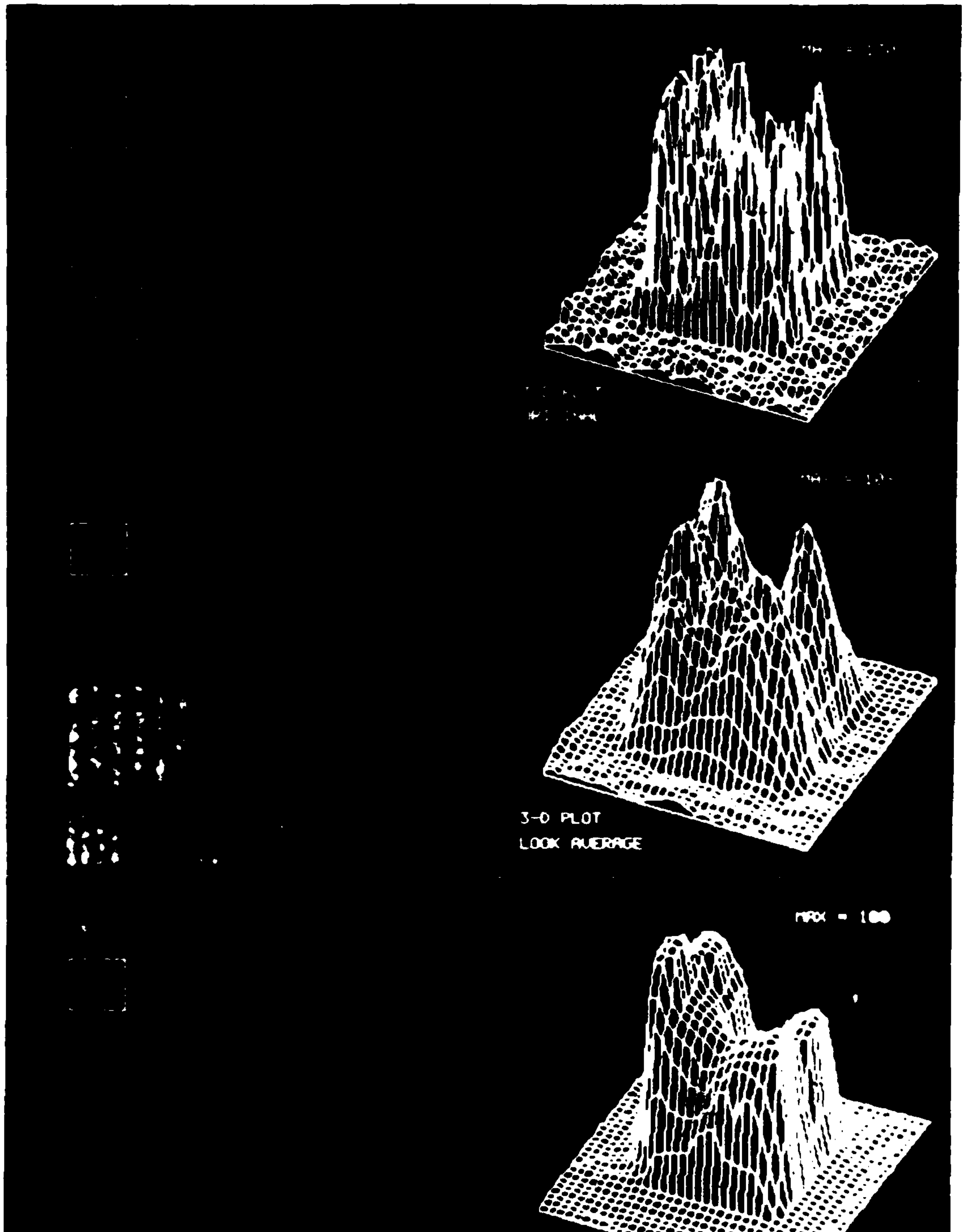

Figure 6. Three-dimensional plots of boxed square.

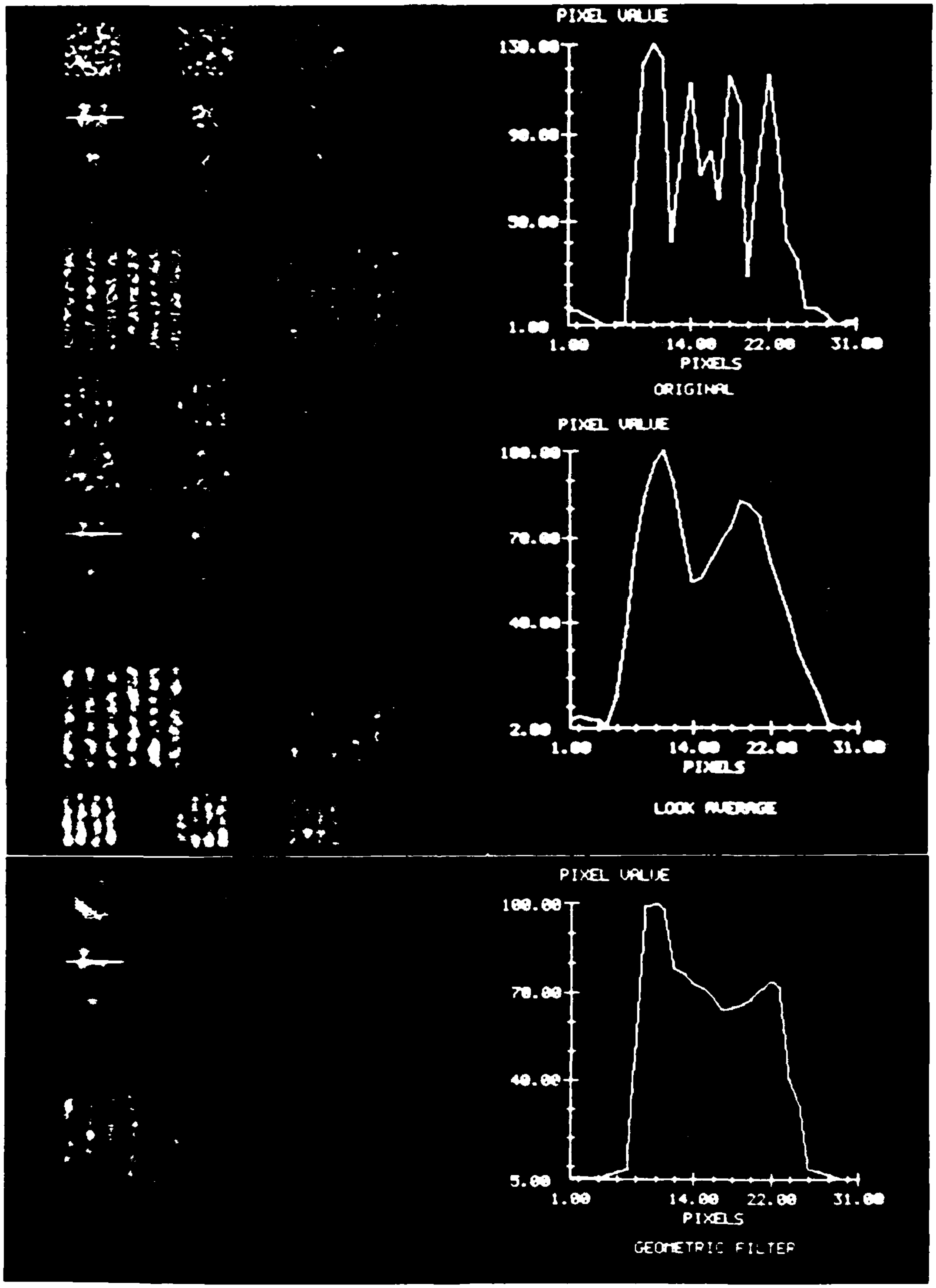

Figure 7. Two-dimensional plots of a slice through a square.

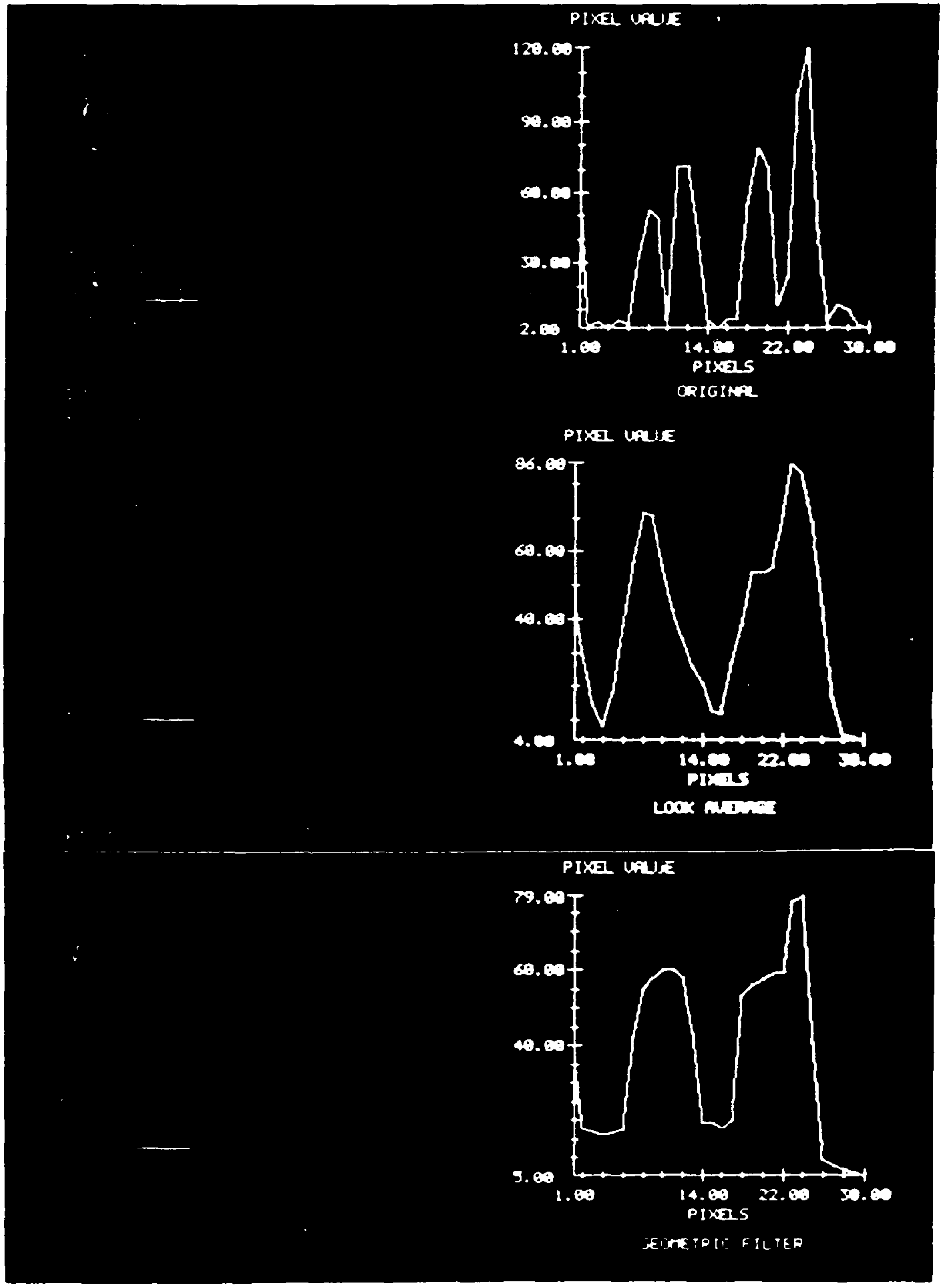

Figure 8. Two-dimensional plots of a slice across part of a grating.

APPENDIX C

"GEOMETRIC FILTER FOR REDUCING SPECKLE"

T. R. Crimmins

Published in Optical Engineering
Vol. 25, No. 5, 651-654 (May 1986)

Geometric filter for reducing speckle

Thomas R. Crimmins
Environmental Research Institute
of Michigan
Radar Division
P.O. Box 8618
Ann Arbor, Michigan 48107

Abstract. *A nonlinear speckle filter based on geometric concepts is defined, and an example of its effectiveness on synthetic aperture radar imagery is shown. Comparison with look-averaging is made using artificial imagery with synthetic speckle.*

Subject terms: speckle; radar; synthetic aperture radar; filter.

Optical Engineering 25(5), 651-654 (May 1986).

CONTENTS

1. INTRODUCTION

The presence of speckle in imagery produced with coherent illumination reduces the detectability of objects in the images.[1-5] It also reduces the effectiveness of some computer algorithms (e.g., edge detection) designed for automatic image analysis.[6]

The geometric filter was designed to reduce speckle in synthetic aperture radar (SAR) imagery while preserving the spatial information in the image such as edges, strong returns, etc. It is an iterative nonlinear algorithm.

2. DEFINITION OF THE GEOMETRIC FILTER

The geometric filter algorithm is based on applying a single iteration of an iterative convex hulling algorithm alternately to the image and to its complement (negative of the image). It is essentially a one-dimensional algorithm that is applied successively in four different directions in the two-dimensional image: horizontal, vertical, and the two diagonal directions.

We will describe the application of the one-dimensional algorithm in the horizontal direction. The image is assumed to have integer gray-level values between 0 and 255.

Each horizontal row of pixels defines a one-dimensional function. The "discrete graph" of this function can be represented by a subset of a discrete grid 256 points high and as many points wide as there are pixels in the horizontal direction of the image. The umbra of the function consists of all points in this grid on or below its discrete graph. One iteration of a convex hulling algorithm is applied to this umbra. (If many iterations were performed, an approximation to the convex hull of the umbra would be formed.) Next, one iteration of this convex hulling algorithm is applied to the complement of the set resulting from the previous step. The output is the function whose umbra is the complement of the set resulting from this last step.

The procedure described above is now applied in each of the other three directions. This constitutes one iteration of the geometric filter.

For a more detailed explanation of the geometric derivation, see Ref. 7 by Crimmins. A program that computes one iteration of the geometric filter is presented in Sec. 8 (the Appendix). This program was implemented on a DeAnza IP 5500 digital video processor using a VAX 11/780 as a host system. Running time is about 14 s per iteration for 512 × 512 images. Usually from 4 to 10 iterations are used.

3. EXAMPLE

Figure 1 is a SAR image of an airport in Windsor, Ontario. It is a four look average[8] made by the STAR-1 airborne SAR system designed and developed by the Environmental Research Institute of Michigan (ERIM). The resolution is 6 m × 6 m, and the pixel spacing is 8.4 m.

Figure 2 shows the result of applying five iterations of the geometric filter. Note that small strong returns retain their sharp edges in the filtered image. Also, medium-contrast edges retain their sharpness, and low-contrast edges are still visible in the filtered image. Figure 3 shows 3-D plots of the boxed small strong return in the original and filtered images. Figure 4 shows similar 3-D plots for the boxed medium-contrast edge.

For measuring the "amount" of speckle reduction, the speckle index is defined in the following way: In view of the multiplicative nature of speckle noise (Goodman,[9] p. 25), the ratio of its deviation to its mean seems to be a reasonable measure of the amount of speckle noise present. For $1 \le m \le M$ and $1 \le n \le N$, we define an approximation to the local deviation by

$$\sigma(m, n) = \max_{-1 \le a, b \le 1} f(m + a, n + b) - \min_{-1 \le a, b \le 1} f(m + a, n + b) , \tag{1}$$

where f is the function representing the image. The local mean is defined as

$$\mu(m, n) = \frac{1}{9} \sum_{a,b=-1}^{1} f(m + a, n + b) \tag{2}$$

The speckle index is then defined by

Invited Paper SO-108 received Oct. 30, 1985; revised manuscript received Jan. 7, 1986; accepted for publication Jan. 7, 1986; received by Managing Editor Feb. 3, 1986. This paper is a revision of Paper 556-30 which was presented at the SPIE International Conference on Speckle, Aug. 20-23, 1985, San Diego, Calif. The paper presented there appears (unrefereed) in SPIE Proceedings Vol. 556.

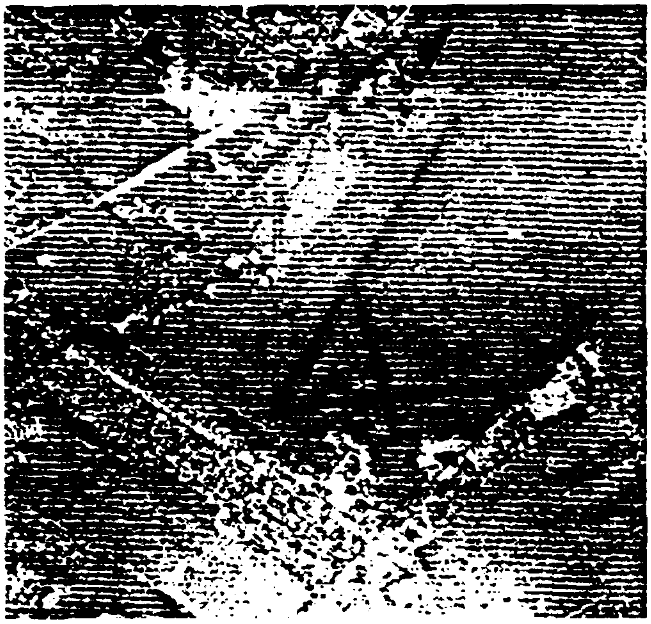

Fig. 1. Original SAR image.

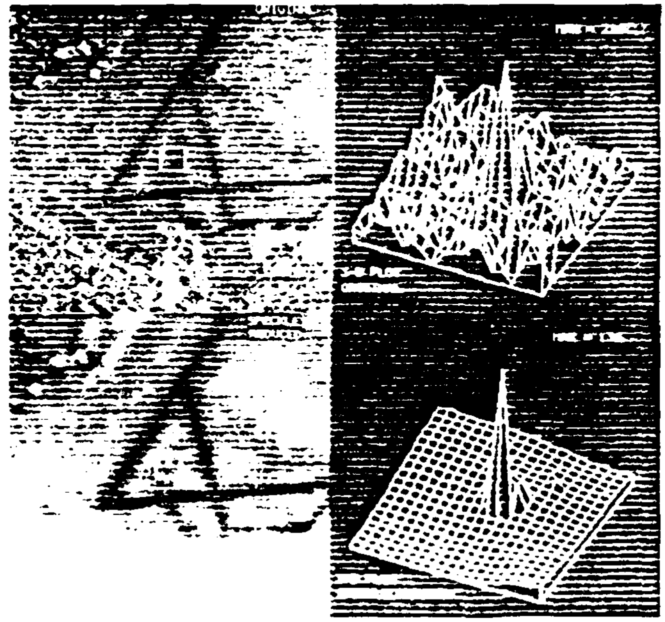

Fig. 3. Three-dimensional plots of a small strong return.

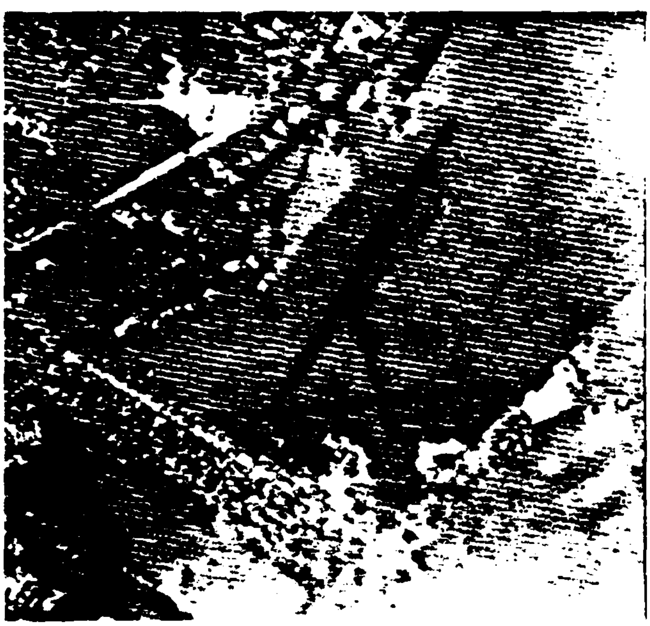

Fig. 2. Result of five iterations of geometric filter.

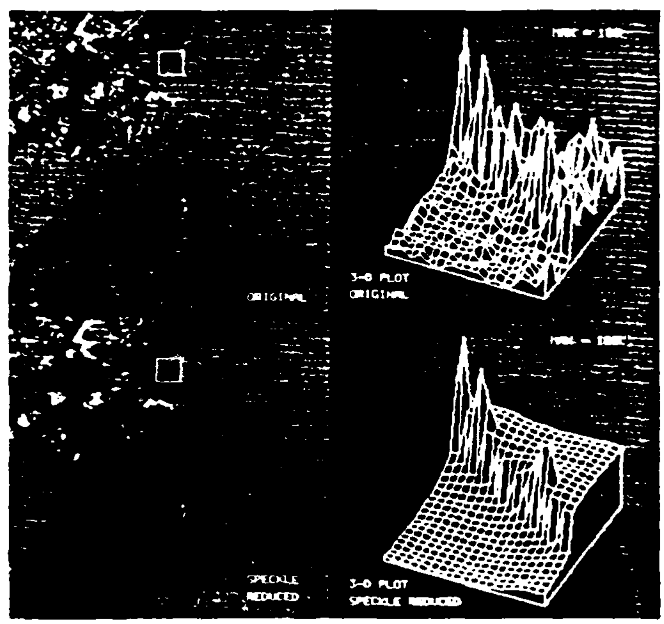

Fig. 4. Three-dimensional plots of a medium-contrast edge.

$$\text{speckle index} \equiv \frac{1}{MN} \sum_{m=1}^{M} \sum_{n=1}^{N} \frac{\sigma(m, n)}{\mu(m, n)} \tag{3}$$

The speckle index for the original image shown in Fig. 1 is 1.05. The filtered image shown in Fig. 2 has a speckle index of 0.36.

4. SYNTHETIC IMAGERY

To create an image with synthetic speckle, we begin by choosing a real-valued image $r(m, n)$ containing some patterns of interest. A random phase image $\phi(m, n)$ is generated where, for each point (m, n), $\phi(m, n)$ is an independent sample from the uniform distribution over the interval from 0 to 2π. We then define a synthetic complex reflectivity function by

$$g(m, n) = r(m, n) \exp[j\phi(m, n)] , \tag{4}$$

where $j = (-1)^{1/2}$. An impulse response function is defined by

$$k(m, n) = \begin{cases} \left(\operatorname{sinc} \frac{\pi}{2} m\right)\left(\operatorname{sinc} \frac{\pi}{2} n\right) & \text{for } m, n \leq 2 , \\ 0 & \text{otherwise} \end{cases} \tag{5}$$

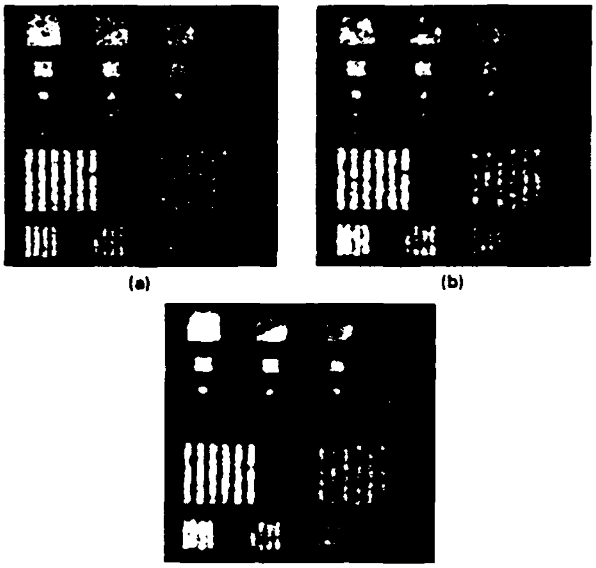

(a) (b) (c)

Fig. 5. (a) Original image with synthetic speckle. (b) Average of four looks. (c) Result of five iterations of geometric filter.

The synthetic complex radar image is defined by $h = k * g$, where * denotes convolution. Finally, the synthetic detected image is defined by $f(m, n) = |h(m, n)|$.

The image $r(m, n)$ used to create the synthetic image in Fig. 5(a) has a background level of 12. It has five rows of squares of sizes 32×32, 16×16, 8×8, 4×4, and 2×2 pixels. The pixel values of the squares, going from left to right, are 170, 130, 90, and 50. The two large gratings consist of bright and dark stripes of dimension 64×6 pixels. The bright stripes have a pixel value of 170 in the first grating and 90 in the second. The dark stripes are at the background level of 12. The stripes in the four smaller gratings have dimension 32×4. The bright stripes have pixel values 170, 130, 90, and 50, and the dark stripes are at the background level of 12.

5. COMPARISON WITH LOOK-AVERAGING

Look-averaging, the noncoherent addition of multiple statistically independent images, is a commonly used technique to reduce speckle noise in SAR imagery and is an obvious reference for comparing the effectiveness of the geometric filter. To make a fair comparison between the geometric filter and look-averaging, the same information was used for both methods.

Look-averaging was carried out as follows. The Fourier transform of the complex image [$h(m, n)$—see the preceding section] was taken, and its square domain was divided into four smaller squares. Each of these four parts of the Fourier transform were then inverse-transformed to obtain four complex looks. The detected looks were obtained by computing the magnitude of the complex looks. Finally, the average of these four detected looks was computed.

The result of this look-averaging process is the image in Fig. 5(b). Figure 5(c) is the result of five iterations of the geometric filter applied to the original image. The speckle indices for these three images are given in Table I.

Figure 6 shows 3-D plots of the boxed square selected from Figs. 5(a) through 5(c), shown top to bottom, respectively.

TABLE I. Speckle Indices for the Images of Fig. 5

Image	Speckle index
Original	0.524
Look-average	0.223
Geometric filter	0.065

Figure 7 shows 2-D plots of a slice through the same square, and Fig. 8 shows 2-D plots of a slice across part of one of the gratings.

It appears from the above that, at least in this case, the geometric filter outperforms look-averaging. Thus, it could be used either to produce higher quality imagery or perhaps to produce imagery of the same quality at a lower cost from fewer data.

6. SUMMARY

The geometric filter has become a standard tool at ERIM for use in processing SAR imagery. It has been found to be useful in preparing imagery both for human inspection and for computer algorithms such as edge detection. It reduces speckle effectively while at the same time preserving the spatial information in the image, e.g., edges and strong returns. This filter appears to outperform the commonly used look-averaging method for reducing speckle.

7. ACKNOWLEDGMENTS

This work was supported by the Army Research Office, Physics Division, under contract DAAG29-84-K-0204.

8. APPENDIX

The image is a function $f(m, n)$ where $1 \le m \le M$, $1 \le n \le N$, and the values of f are integers between 0 and 255. A border of zeros is added to the image so that $f(m, n)$ is defined for $0 \le m \le M + 1$ and $0 \le n \le N + 1$. An auxiliary image $g(m, n)$ is used that is initially set equal to zero on the same extended domain. The following program computes one iteration of the geometric filter.

1. $a \leftarrow 1, b \leftarrow 0, c \leftarrow 3, d \leftarrow 1$.
2. $g(m, n) \leftarrow \max\{f(m, n), \min[f(m-a, n-b) - 1, f(m, n) + 1]\}$, for $1 \le m \le M$, $1 \le n \le N$.
3. $f(m, n) \leftarrow \max\{g(m, n), \min[g(m-a, n-b), g(m, n) + 1, g(m+a, n+b) + 1]\}$, for $1 \le m \le M$, $1 \le n \le N$.
4. If $d = 1$; $a \leftarrow -a, b \leftarrow -b, d \leftarrow 0$, go to 2.
   If $d = 0$; $d \leftarrow 1$, go to 5.
5. $g(m, n) \leftarrow \min\{f(m, n), \max[f(m-a, n-b) + 1, f(m, n) - 1]\}$, for $1 \le m \le M$, $1 \le n \le N$.
6. $f(m, n) \leftarrow \min\{g(m, n), \max[g(m-a, n-b), g(m, n) - 1, g(m+a, n+b) - 1]\}$, for $1 \le m \le M$, $1 \le n \le N$.
7. If $d = 1$; $a \leftarrow -a, b \leftarrow -b, d \leftarrow 0$, go to 5.
   If $d = 0$; $d \leftarrow 1$, go to 8.
8. If $c = 3$; $a \leftarrow 0, b \leftarrow 1, c \leftarrow 2$, go to 2.
   If $c = 2$; $a \leftarrow 1, b \leftarrow 1, c \leftarrow 1$, go to 2.
   If $c = 1$; $a \leftarrow 1, b \leftarrow -1, c \leftarrow 0$, go to 2.
   If $c = 0$; stop.

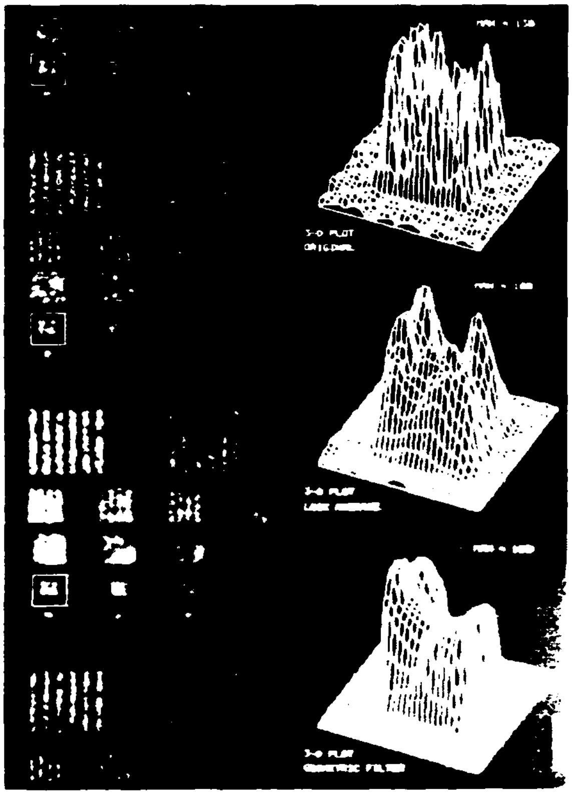

Fig. 6. Three-dimensional plots of boxed square.

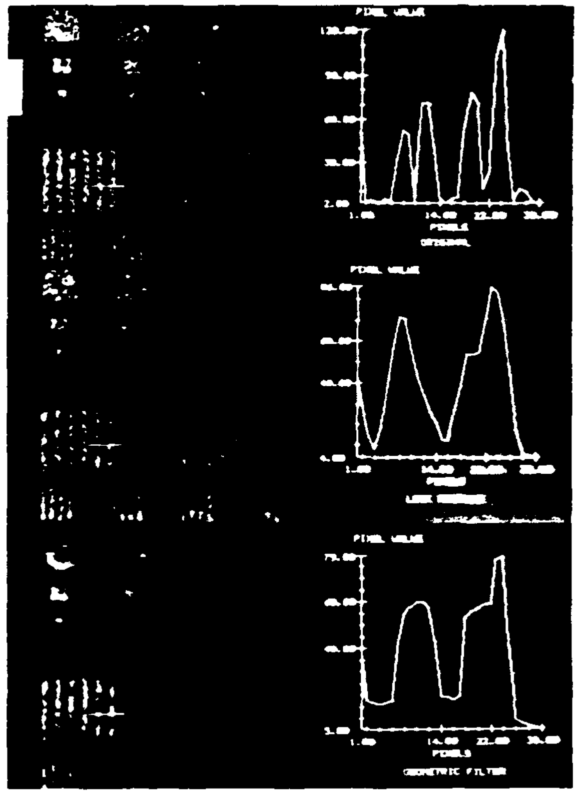

Fig. 8. Two-dimensional plots of a slice across part of a grating.

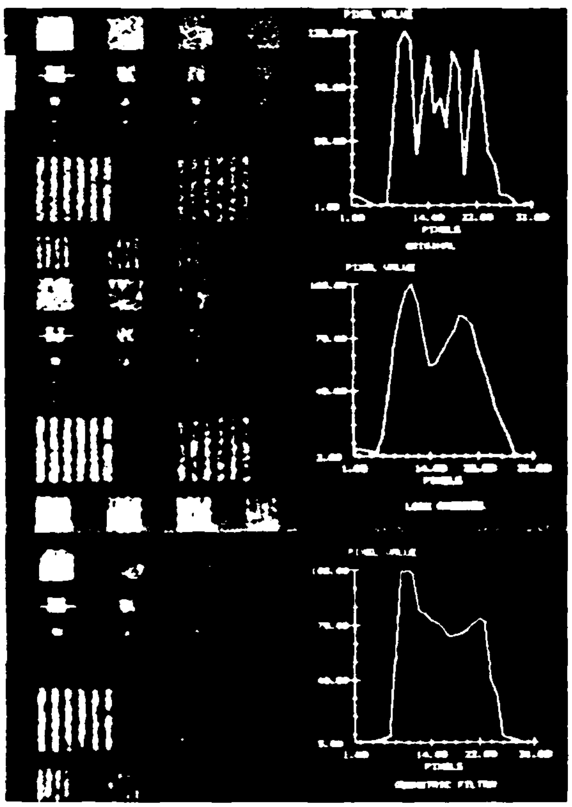

Fig. 7. Two-dimensional plots of a slice through a square.

9. REFERENCES

1. N George, C R Christensen, J S Bennett, and B D Guenther "Speckle noise in displays," J Opt Soc Am 66(11), 1282 (1976)
2. B D Guenther, N George, C R Christensen, and J S Bennett, "Speckle noise and object contrast," Photo Sci and Eng 21, 192 (1977)
3. U N Korwar and J R Pierce, "Detection of gratings and small features in speckle imagery," Appl Opt 20(2), 312 (1981)
4. A Kozma and C R Christensen, "Effects of speckle on resolution," J Opt Soc Am 66(11), 1257 (1976)
5. J L Porcello, N G Massey, R B Innes, and J M Marks, "Speckle reduction in synthetic-aperture radars," J Opt Soc Am 66(11), 1305 (1976)
6. D C Lai, J Potenza, and K Vertaille, "Evaluation of image restoration filters for machine classification," Opt Eng 23(6), 794 (1984)
7. T R Crimmins, "Geometric filter for speckle reduction," Appl Opt 24(10), 1438 (1985)
8. J Zelenka, "Comparison of continuous and discrete mixed-integrator processors," J Opt Soc Am 66(11), 1295 (1976)
9. J W Goodman, "Statistical properties of laser speckle patterns," in *Laser Speckle and Related Phenomena*, J C Dainty, ed, pp 9-75, Springer, Berlin (1984)

Thomas R. Crimmins received the B S degree in mathematics from the University of Detroit, Mich., in 1958 and the M S degree in mathematics from the University of Michigan, Ann Arbor, in 1960

He is presently a research mathematician in the Radar Division of the Environmental Research Institute of Michigan, Ann Arbor, Mich. He has recently worked in the areas of image analysis, edge detection, the phase retrieval problem in optics, synthetic aperture radar, and shape recognition. In the past he has worked in the areas of group codes and functional analysis.

APPENDIX D

PROGRAM FOR THE GENERALIZED GEOMETRIC FILTER

APPENDIX D
PROGRAM FOR THE GENERALIZED GEOMETRIC FILTER

The image is a function $f(j, k)$ where $1 \le j \le J$, $1 \le k \le K$ and the values of f are non-negative integers. A border of zeroes is added to the image so that $f(j, k)$ is defined for $0 \le j \le J + 1$ and $0 \le k \le K + 1$. An auxiliary image $g(j, k)$ is used that is initially set equal to zero on the same extended domain.

The control parameter n is a positive integer and is an input parameter. The following program computes one iteration of the generalized geometric filter.

1. $a \leftarrow 1$, $b \leftarrow 0$, $c \leftarrow 3$, $d \leftarrow 1$.

2. $g(j, k) \leftarrow \max\{f(j, k), \min[f(j - a, k - b) - n, f(j, k) + n]\}$, for $1 \le j \le J$, $1 \le k \le K$.

3. $f(j, k) \leftarrow \max\{g(j, k), \min[g(j - a, k - b), g(j, k) + n, g(j + a, k + b) + n]\}$, for $1 \le j \le J$, $1 \le k \le K$.

4. If $d = 1$; $a \leftarrow -a$, $b \leftarrow -b$, $d \leftarrow 0$, go to 2.
   If $d = 0$; $d \leftarrow 1$, go to 5.

5. $g(j, k) \leftarrow \min\{f(j,k), \max[f(j - a, k - b) + n, f(j, k) - n]\}$, for $1 \le j \le J$, $1 \le k \le K$.

6. $f(j,k) \leftarrow \min\{g(j, k), \max[g(j - a, k - b), g(j, k) - n, g(j + a, k + b) - n]\}$, for $1 \le j \le J$, $1 \le k \le K$.

7. If $d = 1$; $a \leftarrow -a$, $b \leftarrow -b$, $d \leftarrow 0$, go to 5.
   If $d = 0$; $d \leftarrow 1$, go to 8.

8. If $c = 3$; $a \leftarrow 0$, $b \leftarrow 1$, $c \leftarrow 2$, go to 2.
   If $c = 2$; $a \leftarrow 1$, $b \leftarrow 1$, $c \leftarrow 1$, go to 2.
   If $c = 1$; $a \leftarrow 1$, $b \leftarrow -1$, $c \leftarrow 0$, go to 2.
   If $c = 0$; stop.

END

1-87

DTIC